Histol Histopathol (2024) 39: 573-593

Histology and Histopathology
From Cell Biology to Tissue Engineering

ORIGINAL ARTICLE Open Access

Heterogeneity of mesenchymal cells in human amniotic membrane at term

Salvador Cortes-Sandoval[1,2*], Vicente Seco-Rovira[2*], Ester Beltrán-Frutos[2*], María I. Serrano-Sánchez[2], Jesús Martínez-Hernández[2], Concepción Ferrer[2], Juan L. Delgado[1], Carmen L. Insausti[3], Miguel Blanquer[3] and Luis M. Pastor[2]

[1]Department of Obstetrics and Gynecology, Virgen de la Arrixaca Hospital, IMIB, [2]Department of Cell Biology and Histology, IMIB, School of Medicine, Regional Campus of International Excellence "Campus Mare Nostrum", University of Murcia and [3]Hematology Service, Virgen de la Arrixaca University Hospital, IMIB, Murcia, Spain

*These authors contributed equally to this work

Summary. There is increasing interest in understanding the tissue biology of human amniotic membrane (hAM) given its applications in medicine. One cellular component is mesenchymal cells, which can be extracted, cultured and differentiated "*in vitro*" into various cell types. These studies show that there is heterogeneity among mesenchymal cells. The aim of this work is to study the membrane "*in situ*" to determine whether this cellular heterogeneity exists. The hAMs were obtained from caesarean deliveries at term and analyzed by histological techniques. Types I-III mesenchymal cells and Hofbauer were distinguished by light microscopy. Histochemically, mesenchymal cell types showed successively increasing positivity to: PAS, vimentin, fibronectin, and Concanavalin-A; VGEF, TGF-β2, PDGF-C, FGF-2. By the semiquantitative point of view, the percentage of Type II cells was 60%, significantly higher than the other types. With transmission electron microscopy, an intermediate cell type between II-III was observed. Strong vesiculation of the rough endoplasmic reticulum (RER) with exocytosis was observed. In addition, an accumulation of a similar material to the extracellular matrix in the RER caused its dilation especially in type III_{TEM} cells. Some of this material acquired a globular structure. These structures were also found free in the extracellular matrix. In conclusion, the mesenchymal cells of the fibroblastic layer of the hAMs studied are heterogeneous, with some undifferentiated and others with a probably senescent fibroblastic phenotype with accumulation in their RER of fibronectin. These results may be of interest to extract mesenchymal cells from hAMs for use in regenerative medicine and to better understand the mechanisms of fetal membrane rupture.

Key words: Heterogeneity, Mesenchymal cells, Fibroblast layer, Fibronectin, Human amniotic membrane

Corresponding Author: Dr. Luis Miguel Pastor, Department of Cell Biology and Histology, IMIB-Arrixaca, School of Medicine, University of Murcia, Avda. Buenavista s/n. 30120 El Palmar, Murcia, Spain. e-mail: bioetica@um.es

www.hh.um.es. DOI: 10.14670/HH-18-660

Introduction

Human amniotic membrane (hAM) and chorion constitute the fetal placental membranes whose function is to provide a safe environment for embryonic development (Jones and Jauniaux, 1995; Kobayashi et al., 2009). The hAM has two known embryological origins: the amniotic epithelium, derived from the epiblast, and the mesenchymal stroma, derived from the hypoblast, which form the extraembryonic mesoderm 12 days after fertilization (Parolini et al., 2008; Insausti et al., 2010). This histological structure has been extensively described (Toda et al., 2007; Insausti et al., 2010) and is composed by two different tissue elements, the amniotic epithelium, and the extraembryonic mesoderm. This mesoderm is composed of a layer of extracellular matrix without cells called compact layer, a fibroblastic layer, and a spongy layer. The fibroblastic layer consists of an extracellular matrix with some collagen fibers and numerous mesenchymal cells, as well as some macrophagic cells (Hofbauer cells) (Fakonti et al., 2022).

In recent decades, advances in the understanding of the hAM have led to the development of therapeutic applications in the field of ophthalmology and in the healing of complex wounds such as diabetic ulcers, burns, etc (Toda et al., 2007). In particular, human amniotic membrane mesenchymal cells (hAMSC) have aroused interest for their application in regenerative medicine due to their immunogenic characteristics, their

high "*in vitro*" expansion capacity, their self-regenerative capacity and for being an easily accessible source of stem cells that avoids the major ethical problems associated with the use of stem cells of embryological origin (Toda et al., 2007; Sessarego et al., 2008; Insausti et al., 2010). A classic example of mesenchymal cell application from the amniotic membrane is its possible use in cardiac regeneration. Several studies have assessed the current evidence from preclinical investigations on the application of these cells in the treatment of ischemic cardiomyopathies, including myocardial ischemia and heart failure (Gorjipour et al., 2021; Shen et al., 2021)

The isolation and culture of hAMSCs has revealed a great capacity to differentiate into cells of any lineage: ectodermal (neurons), mesodermal (cardiomyocytes, musculoskeletal cells, endothelial cells, etc.) and endodermal (pancreatic or hepatic cells) (Alviano et al., 2007). Furthermore, it has been observed that hAMSCs acquired different morphological characteristics depending on the cell line to which they were differentiated "*in vitro*" (In ´t Anker et al., 2004; Portmann-Lanz et al., 2006). At the same time, it has been possible to determine that the self-regenerative capacity, the number of culture passages, the growth rate and the affinity to differentiate into certain cell types are influenced by the weeks of gestation at which they were obtained, although there is still no clear explanation for this relationship (In 't Anker et al., 2004; Portmann-Lanz et al., 2006).

Most of the knowledge about hAMSC cells that we have today dates back to the brief descriptions made in the middle of the last century on placentas from the first and second trimester of pregnancy. (Jones and Jauniaux, 1995). More recent are the studies about these cells, "*in vitro*" even at an ultrastructural level (Pasquinelli et al., 2007). However, there do not seem to be studies that histologically characterize these cells in hAM at term "*in vivo*". Doing so could be of interest as different types might be found in them that may be related to their viability for culture or their potential to differentiate in diverse tissues. These studies could also be of interest to better understand the changes that occur in fetal membranes during childbirth.

Just as there are changes at the molecular level in fetal membranes that indicate their maturation or senescence at the end of pregnancy (Behnia et al., 2015; Menon, 2016) and facilitate their rupture (Méhats et al., 2011; Strauss, 2013), it is very likely that these changes also affect hAM cells. Therefore, it should be considered that specific signs and characteristics might be observed in the mesenchymal cell population related to the differentiation or senescent state assigned with fetal membranes at term. Consequently, with all of the above, our work has the following objectives: a) to characterize the mesenchymal cell population of the hAM of placentas at term by light and electron microscopy, b) to analyze and determine the frequency of the possible hAM cell types found and c) to perform immunohistochemistry of various markers proteins on these different types of mesenchymal cells that can correlate their morphological characteristics with different functionality.

Materials and methods

Acquisition of amniotic membrane

This study was approved by the local ethics committee (University Hospital Vírgen de la Arrixaca, Murcia, Spain), the Spanish Agency of Medicines and Medical Devices (AEMPS) and was conducted after obtaining written informed consent from the hAM donors.

Processing and preparation of hAMs

Fetal membranes were obtained from healthy women (n=5) after uncomplicated cesarean sections between 37-40 weeks of pregnancy. Amniotic membrane sections were specifically collected from the peri-umbilical cord area. They were washed in 1,000mL of physiological saline solution (PSS), one part of the membrane was placed in paraformaldehyde (4%) for 8 hours before being submitted to light microscopy study, and the other was used for transmission electron microscopy (TEM). The samples were dehydrated, immersed in toluene and embedded in Paraplas plus (Panreac, Quimica SA, Barcelona, Spain). Sections 5 µm thick were stained with hematoxylin and eosin (H&E).

Conventional carbohydrate techniques and lectin histochemistry

The sections were processed by PAS (Periodic Acid Schiff), Alcian Blue to pH=2.5 and pH=1; (AB pH=2.5) and (pH=1)) (Calvo et al., 1995). For lectin histochemistry, sections were deparaffinized and rehydrated through a series of decreasing concentrations of ethanol. After a brief rinse for 5 min in TBS (Tris buffered saline, pH 7.4), slides were incubated in a solution containing 0.3% H_2O_2 to block endogenous peroxidase activity. After 3 rinses in TBS, sections were incubated with HRP-lectins (PNA, Con-A, WGA) SIGMA (St. Louis MO, USA) at the appropriate dilution in a humidity chamber at room temperature for 1.5h. After washing in TBS, the sections were immersed in TBS containing 0.05% DAB and 0.3% H_2O_2 to demonstrate peroxidase-containing sites. The sections were then counterstained with Harris hematoxylin, dehydrated, cleared and mounted in DPX. To assess the specificity of lectin staining, the following controls were used: (1) preabsorption of the lectins with their corresponding inhibitory sugar at a concentration of 0.2 M; and (2) substitution of the conjugated lectin by TBS to determine the presence of endogenous peroxidase activity (Pinart et al., 2001).

Immunohistochemistry

Different sections of amniotic membrane were deparaffinized and rehydrated and subsequently incubated overnight at 4°C with Santa Cruz antibodies, anti-VEGF [C-1] (sc-7269), anti-TGF-β2 [V] (sc-90), anti -PDGF-C [C-17] (sc-18228), anti-FGF-2 [147], (sc-79), anti-TGF-β1 [TB21] (sc-52893), anti-Flg [C-15] (sc-121), anti-IGF-1 [H-70] (sc-9013), anti-fibronectin [C-20] (sc-6952), anti-HSP-47 [H-300] (sc- 8352), anti-laminin β2 [H-300] (sc-20777), anti-connexin 43 [D-7] (sc-13558), anti-α-Actin [1A4] (sc-32251), and anti-vimentin [Dako Clone V9] (M 0725) in a solution containing TBS with 1% BSA. Subsequently, the sections were washed in PBS and incubated for 45 minutes at room temperature with biotinylated goat anti-rabbit antibodies (Chemicon International, AP1323), biotinylated rabbit anti-goat antibodies (Dako, Denmark), and biotinylated rabbit anti-mouse antibodies (Dako, Denmark) at concentrations of 1:200 in 1% PBS-BSA. Subsequently, slides were incubated in straptavidin (Dako, Denmark) 1:300. The antibody-peroxidase complex was developed with 0.05% diaminobenzidine and 3% hydrogen peroxide. The specificity of the immunohistochemical techniques was confirmed in sections incubated with non-immune serum instead of the primary antibody.

Transmission electron microscopy (TEM)

Samples (1 mm^3) were fixed for 4h in 3.5% glutaraldehyde in 0.1M sodium cacodylate buffer. They were then washed in 0.855 mg/100mL saccharose cacodylate, postfixed in 1% osmium tetroxide (for 2h), dehydrated in a graded acetone series and embedded in Epon 812 (Serva, Heidelberg, Germany). Semithin sections (1 μm) were stained with toluidine blue. Ultrathin sections (90-120 nm) were cut with a Reichert-Imy Ultracut ultramicrotome, contrasted with uranyl acetate and lead citrate and examined with a Philips TECNAI 12 transmission electron microscope.

Semiquantitative light microscopy study of mesenchymal cell types

Cell counting of mesenchymal cell types of the fibroblastic layer was performed on 4 random semithin sections of each membrane using an Olympus BX51 microscope. To differentiate each cell type, the nuclear and cytoplasmic characteristics were taken into account (type I, contains a large, homogeneous and euchromatinous nucleus with little cytoplasmic content; type II, irregular and spindle-shaped nucleus with perinuclear heterochromatin, elongated cytoplasm with numerous globular structures and dilations cytoplasmic; type III, small, irregular, heterochromatic nucleus, elongated cytoplasm occupied by large globular vacuoles; type IV, irregular nucleus and very thin and long cytoplasmic prolongations). The population index of each cell type (I, II, III and IV) was calculated in relation to the total number of all cell types and multiplied by 100 to obtain the percentage.

Semiquantitative study with transmission electron microscopy

A minimum of 3 ultrathin sections from each of the hAM were used. In this study, the technique made it possible to distinguish 5 types of mesenchymal cells being able to better differentiate their organelles. Thus, they were differentiated into type I_{TEM}, large, rounded euchromatic nucleus with poorly differentiated cytoplasm and large mitochondria; type II_{TEM}, irregular nucleus with rough endoplasmic reticulum (RER) and incipient vesicles and small mitochondria; type III_{TEM}, irregular nucleus with perinuclear heterochromatin, abundant and dilated RER, small mitochondria and considerable vesicles; type IV_{TEM}, irregularly contoured nucleus with scattered euchromatin and large RER dilations occupying most of the cytoplasm; type V_{TEM} similar to light microscopy type IV with abundant lysosomes in the cytoplasm. The number of each cell type was calculated relative to total number of all cell types and multiplied by 100 to obtain the percentage. To visually count, all the mesenchymal cells contained in the fibroblastic layer of the ultrathin sections of each membrane were taken into account.

Statistical analysis

The statistical study of the indices of each cell type performed on semithin sections was carried out by an analysis of variance followed by a post hoc test comparing the equality between pairs of means using the DMS test and the Bonferroni method. Results were considered statistically significant at values $p<0.05$. For the statistical evaluation of cell heterogeneity in ultrathin sections, the contrast of a distribution of cell types was used, admitting an identical distribution for each of the types. Statistically significant results are those with residuals <-2 or >2. The SPSS 28 (IBM Corporation, Armonk, NY) statistical software package was used.

Results

Light microscopy

In the sections embedded in paraffin, the different tissue zones already known from the hAM were observed: a) an uninterrupted band of epithelial cells and b) a band of avascular extraembryonic mesoderm. In the latter, the compact, fibroblastic and spongy layers were differentiated (Fig. 1a). In the fibroblastic layer it was possible to identify a heterogeneous population of mesenchymal cells that were distributed parallel to the epithelium in one or several rows. Occasionally, clusters of cells were observed near each other. Morphologically,

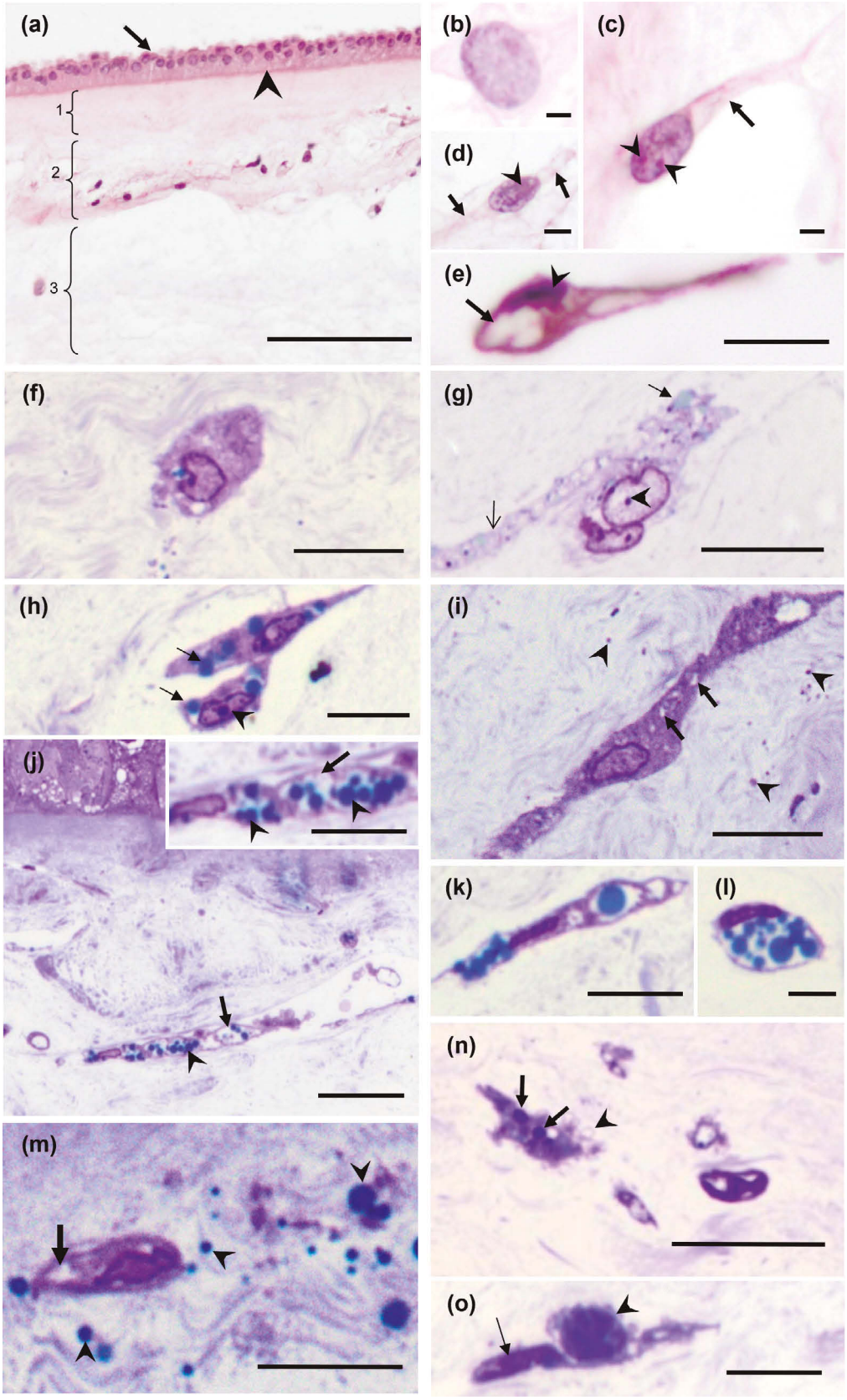

Fig. 1. a-e. Hematoxylin-eosin sections: **a.** hAM layers. Amniotic epithelium (arrow), basement membrane (arrowhead) and amniotic mesoderm: compact layer (1), fibroblastic layer (2) and spongy layer (3). **b.** Type I cell with euchromatin nucleus and scant cytoplasm. **c, d.** Type II cells with perinuclear heterochromatin and nucleoli (arrowheads). Cytoplasmic processes (arrows). Incipient intracytoplasmic dilatations (thin arrow). **e.** Longitudinal section of the nucleus of type III cells (open arrow). Intracytoplasmic globular dilatations (arrow). **f, g.** Semithin sections stained with toluidine blue: **f.** Type I cell with some small deposits reactive to toluidine blue. **g.** Type II cell with a large oval nucleus and central nucleolus (arrowhead), cytoplasmic extension (thin arrow) with small intracytoplasmic globular dilatations inside and weakly stained deposits (arrow). **h.** Type II cells at a more advanced stage in their evolution where most heterochromatinic nucleus and a well-differentiated nucleolus are observed (arrowhead). In addition, more abundant, larger, and more intensely colored intracytoplasmic deposits are observed (arrows). **i.** Type II cell. Dilatation in cytoplasm reticulum (arrows). In extracellular matrix small globular structures (arrow heads). **j.** Type III cell in an advanced stage where a large dilation is observed (arrow) with a large number of intracytoplasmic deposits inside (arrowhead). The insert shows a detail of the cell showing the large dilations (arrow) occupied by reactive globular structures (arrowhead). **k, l.** Longitudinal **(k)** and transversal **(l)** sections, respectively, of type III cells in which the cytoplasm is almost entirely occupied by large dilations containing large and numerous reactive globular structures. **m.** Free globular structures stained intensely with toluidine blue (arrowhead) in the extracellular matrix close to the mesenchymal cells (arrow). **n.** Hofbauer cell with fine and long cytoplasmic projections (arrowhead) and numerous cytoplasmic vacuoles (arrows). **o.** Hofbauer cell (arrowhead) in close contact with a type III cell (arrow), a frequently observed phenomenon. Scale bars: a, 200 μm; b, c, 2 μm; d, l, 5 μm; e, 4 μm; f-i, k, inserts k, o, 10 μm; j, n, 25 μm; m, 20 μm.

these cells were characterized and classified into three types: type I, with a rounded euchromatic nucleus and little cytoplasm content surrounding the nucleus (Fig. 1b); type II, with a nucleus with an irregular contour, often oval or spindle-shaped and more heterochromatinous than type I cells. The cytoplasm of some of them showed incipient prolongations, while others had a clear spindle-shaped and elongated morphology. On the inside of the cytoplasm, small intracytoplasmic accumulations could be observed that did not show affinity to H&E (Fig. 1c,d); type III, with an elongated nucleus of small diameter, highly hyperchromatic. Its cytoplasm was divided into two opposing long processes with respect to the cytoplasm surrounding the nucleus. Within the cytoplasm, globular structures of material that did not show affinity for H&E were often observed (Fig. 1e). The semithin sections (Fig. 1f-o) facilitated a more detailed morphological characterization, which allowed mesenchymal cells to be classified into four types: type I, with a large, spherical, euchromatic nucleus with a regular contour. This cell did not present prolongations and inner small globular structures stained in light blue color were rarely observed (Fig. 1f). Occasionally it was possible to appreciate that this cell type was sometimes organized in a grouped manner, forming a certain cellular niche; type II included cells whose nuclei presented oval morphology with little or moderate heterochromatin content, mainly adjacent to the nuclear membrane and occasionally with a nucleolus and cells with nuclei of clearly fusiform and irregular morphology, with marked heterochromatinic content, irregularly distributed throughout the nucleus, although predominantly in the area adjacent to the nuclear membrane. The cytoplasm of some cells of this type showed incipient prolongations, while on other occasions, they adopted a spindle-shaped morphology with long prolongations. In the cytoplasmic interior, abundant accumulations of globular structures stained in light blue could be observed (Fig. 1g-i). Small globular structures were also observed in the extracellular matrix close to the mesenchymal cells (Fig. 1i); type III, with spindle-shaped nuclei with irregular contour and intense heterochromatin. The cytoplasm was found surrounding the nucleus and in two opposing long processes. Inside the cytoplasm there were wide dilatations with globular structures, sometimes large, light blue stained. Near these mesenchymal cells, globular structures strongly stained by toluidine blue were more frequently observed, and the surrounding extracellular matrix showed faint staining (Fig. 1j-m). Type IV, cells with an irregularly contoured nucleus with moderate scattered heterochromatin arranged in the nucleus. The cytoplasm contained some globular structures with various shades of blue. The contour of the cytoplasm was irregular and had numerous long and thin cytoplasmic processes concluding that their morphology coincided with that of Hofbauer cells (Fig. 1n-o). It was common to find these cells in close contact with type II and III cells (Fig. 1o).

Conventional carbohydrate techniques and lectin histochemistry

Using the PAS technique (Fig. 2a-g), a marked difference was observed in the staining pattern of type III cells compared to type I and II cells. It was evident that type I cells had a cytoplasm with small positive globular structures (Fig. 2a). In type II cells it was already possible to find accumulations, sometimes large, of positive globular structures, irregularly distributed throughout the cytoplasm, although this phenomenon was not observed in all cells (Fig. 2b-d). In type III cells, a greater positivity was found than in the previous cell types. The cytoplasm was intensely positive, with small absent areas of positivity (Fig. 2e-g). In the proximal extracellular matrix, especially of type III cells, PAS-positive globular structures were identified (Fig. 2g). Alcian blue pH 2.5 showed strong positivity throughout the entire amniotic membrane mesoderm. Mesenchymal cells showed little or no positivity in their cytoplasm, which allowed the identification of globular structures without positivity in some types of these cells. In particular, unstained perinuclear dilations occupying a large part of the cytoplasm, especially in type II and III cells were observed (Fig. 2h). Regarding the three lectins used, only Concanavalin-A showed positivity in mesenchymal cells, being very weak or negative in Type I cells (Fig. 2i) but increasing in types II and III cells, being more intense in type III cells (Fig. 2j,k). Characteristically, the positivity was very intense and located in globular structures of different sizes, although diffuse positivity could also be observed in the cytoplasm, revealing negative circular cytoplasmic spaces.

Immunohistochemistry

The immunohistochemical results obtained for the different proteins analyzed are summarized in Table 1. Regarding the extracellular matrix proteins, it was possible to identify fibronectin in the three cell types (Fig. 2l-n), although its distribution was heterogeneous. In type I cells it showed a weak-moderate intensity, in type II cells moderately intense and in type III cell intense. For its part, the cytoplasmic distribution presented a homogeneous arrangement throughout the cytoplasm, but also irregularly distributed intracytoplasmic globular structures were found with very strong positivity (Fig. 2m,n). Regarding vimentin positivity, it was found in all three cell types, although the intensity of positivity was variable, being mild in type I, moderate-intense in type II and very intense in type III. Vimentin positivity was homogeneous throughout the cytoplasm, but many cells showed circular gaps absent of positivity (Fig. 3a,b). The positivity to α-actin was more variable, in type I cells it was frequently negative or slightly positive, while in type II and III cells the positivity increased along with

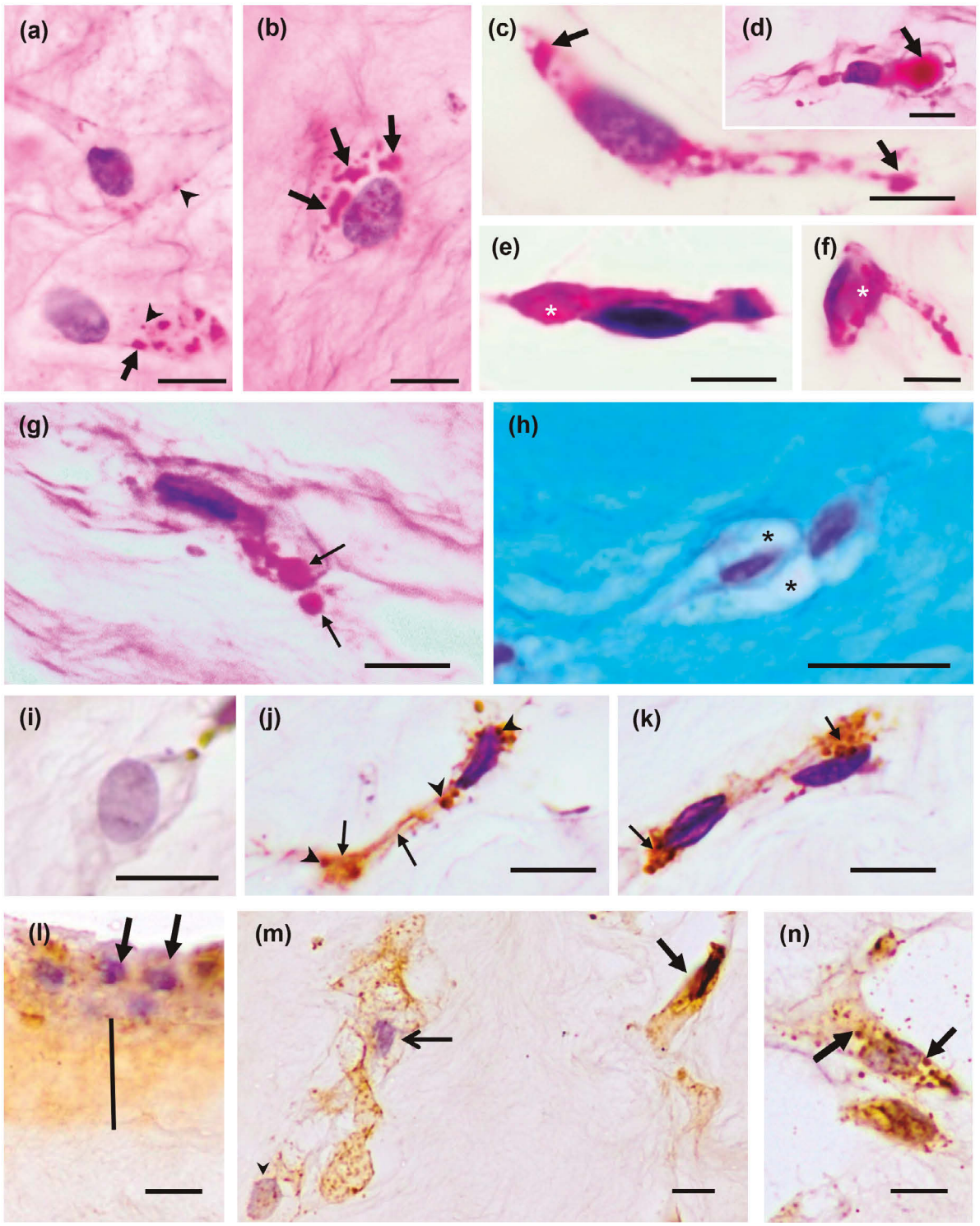

Fig. 2. a-g. PAS histochemical staining technique. Progressive accumulation of cytoplasmic deposits from type I to type III cells were observed: **a.** Type I cell with very small deposits (arrowheads) and medium-sized deposits (arrow). **b.** Incipient type II cell with accumulations of considerable size (arrows). **c.** Type II cell with deposits of PAS-positive material (arrows) that occupy most of the cytoplasm. **d.** Advanced type II cell with a large dilation occupied by PAS-positive material (arrow). **e, f.** Longitudinal **(e)** and transversal **(f)** section of type III cells showing cytoplasm filled with PAS-positive material (asterisks). **g.** Globular deposits of PAS-positive material in the extracellular matrix near the cells (short arrow) and inside the cytoplasm (long arrow). **h.** Alcian blue pH 2,5 histochemical technique: mesenchymal cells with negative and clear cytoplasm (asterisks) can be observed. **i-k.** Histochemical technique of the concanavalin A lectin. **i.** Type I cell negative for this lectin. **j.** Type III cells with diffuse cytoplasmic positivity (arrows) together but organized mainly in globular concretions (arrowheads). **k.** Type III cells with large positive globular deposits (arrows). **l-n.** Fibronectin immunohistochemical technique. **l.** hAM with epithelial cells (arrows) being observed below the intensely positive compact layer (bar). **m.** Type I cell (arrowhead), type II (open arrow) and a type III cell (closed arrow) where cytoplasmic positivity is observed to increase in each of them respectively. **n.** Detail of a type II cell where globular bodies are clearly visible. Scale bars: a-g, i-n, 10 μm; h, 50 μm.

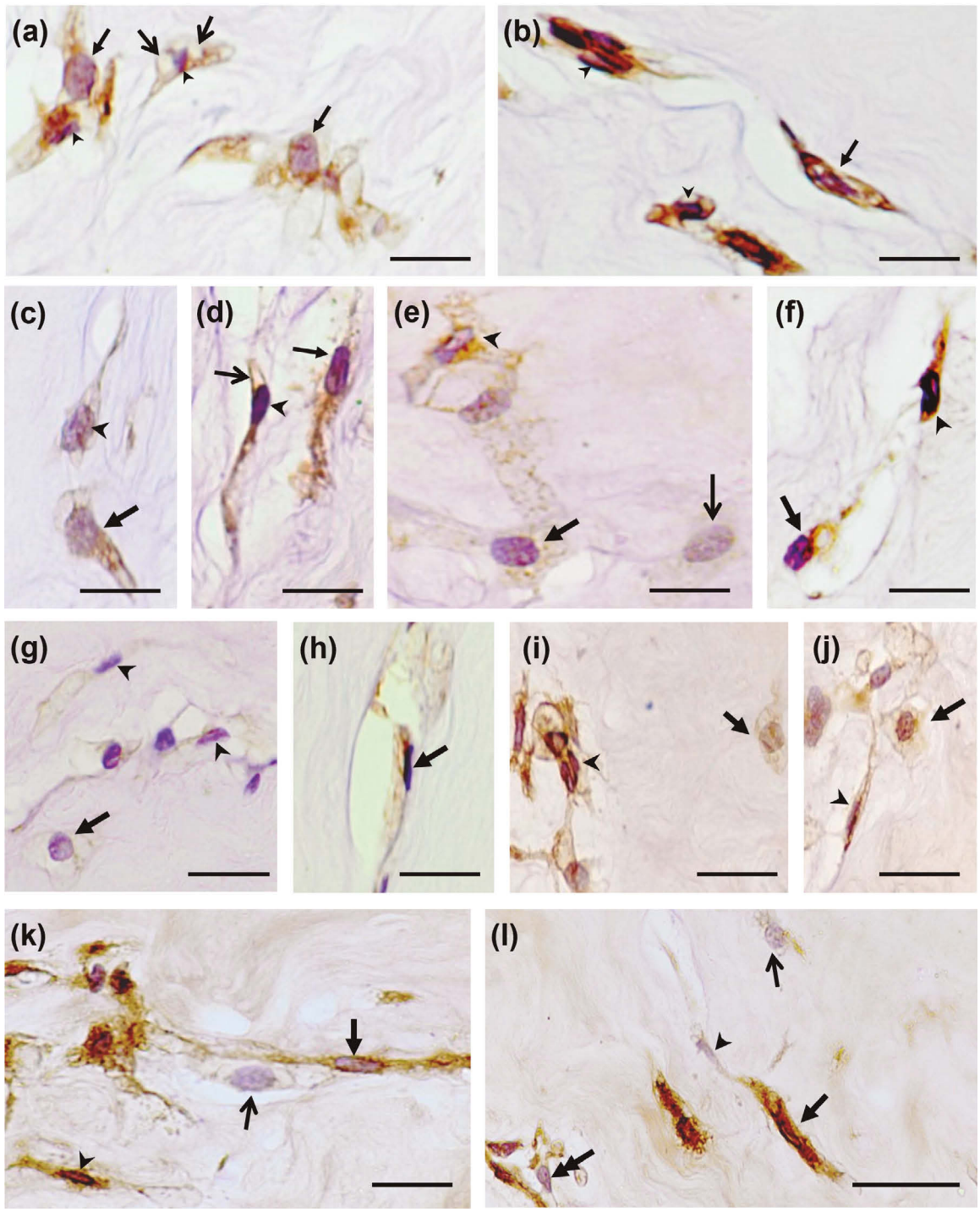

Fig. 3. Immunohistochemistry techniques for several proteins and growth factors expressed by the different stem cells identified. **a, b.** Immunohistochemistry for Vimentin. **a.** Type I cells (arrows) showing positivity in their cytoplasm and intense positivity in type III cells (arrowhead). Cytoplasmic empty circular spaces are observed in all types (open-headed arrow). **b.** An intensely positive type II cell (arrow) and several intensely positive type III cells (arrowhead) stand out. **c, d.** Immunohistochemistry for VEGF. **c.** VEGF-positive type 1 cell (arrow) and non-VEGF-positive type 1 cell (arrowhead). **d.** Type II cell positive for VEGF (arrow) and type III cell intensely positive for VEGF (arrowhead) where non-positive circular cytoplasmic spaces are observed (open-headed arrow). **e, f.** Immunohistochemistry for PDGF-C. **e.** Type I cells negative for PDGF-C (open-headed arrow), type I cell slightly positive (arrow) and type II cell positive (arrowhead). **f.** Type II cell positive (arrow) and highly positive type III cell (arrowhead). **g, h.** Immunohistochemistry for α-actin. **g.** Cell types I (arrow) and II (arrowhead) show little positivity. **h.** Type III positive cells (arrows) are observed. **i, j.** Immunohistochemistry for connexin 43. **i.** Type I cell (arrow) with little cytoplasmic positivity and type III cell intensely positive (arrowhead). **j.** Type II cell moderately positive (arrow) and intensely positive type III cell with clearly spindle-shaped morphology (arrowhead). **k.** Immunohistochemistry for TGF-β2. A negative type I cell (open-headed arrow), a moderately intense type II cell (arrow), and a very intense type III cell (arrowhead) are observed. **l.** Immunohistochemistry for FGF-2. A negative type I cell (open-headed arrow), a moderately positive type II cell (arrow), and a type III cell (double arrow) with intensely positive cytoplasmic are observed. Scale bars: a-f, h-k, 10 μm; g, 40 μm; l, 20 μm.

negative cells (Fig. 3c,d). Connexin 43, which is part of the gap junctions, was identified in all mesenchymal cell types, but with graded intensity. Thus, type I cells were slightly or moderately positive, type II cells moderated positive and type III cells strongly positive. Cytoplasmic positivity left circularly non-positive circumscribed areas (Fig. 3e,f). The growth factors studied showed an increasing intensity of staining in the cytoplasm from type I to type III cells. Thus, it was observed that for type I cells: the factors VGEF, FGF-2, TGFβ-2 and PDGF-C were in some cells weakly positive being TGFβ-2 the which showed the most intense positivity. For type II, the factors VGEF, FGF-2, TGFβ-2 and PDGF-C were positive, with TGFβ-2 being again the most intense. Finally, in type III cells, strong staining intensity was observed for VGF, FGF-2, TGFβ-2 and PDGF-C. TGFβ-1, Flg and IGF-1 were negative in all mesenchymal cell types (Fig. 3g-l). As for HSP-47 protein, its presence in all cell types was generally negative, although it was possible to find weakly positive type II and III cells. Lastly, Laminin β2 was negative in all mesenchymal cell types.

Transmission electron microscopy

This technique allowed a greater morphological definition in the study of mesenchymal cells, which led to distinguish up to five cell types. Type I_{TEM}, are cells with a large rounded euchromatic nucleus with a nucleus/cytoplasm ratio close to unity. The cytoplasmic content was scarce, there were large mitochondria with the presence of dense granules inside and a moderately dense matrix. The RER and Golgi complex were poorly developed (Fig. 4a,b). Type II_{TEM}, cells had euchromatic nuclei with indentations and irregular contour. The cytoplasmic content was increased, especially in the form of two cytoplasmic projections oriented along the axis of the nucleus. In the cytoplasm, a large content of RER distributed throughout it was found. Along with the cisterns, small reticulum vesicles containing low-electrodensity material were also observed. Also, numerous strongly electron-dense and small mitochondria were found, characteristically arranged at both poles of the nucleus (Fig. 4c,d). Type III_{TEM}, cells had an irregular, mainly elongated nucleus with heterochromatic content, mostly perinuclear in arrangement and frequently with a nucleolus. The cytoplasm presented clear extensions in the longitudinal axis of the nucleus, giving the cell a spindle-shaped morphology. Most of the cell organelles were located at both poles of the nucleus: small, electron-dense mitochondria were found in variable numbers, as well as a very abundant RER. Characteristically, this was observed to be moderately dilated and even very dilated at times. The content presented a material with low electron density and a texture with characteristics like those observed in the extracellular matrix surrounding the cell. When these dilations of the RER reached a larger size, the formation of areas with higher electron density could be observed inside them. In some locations of the plasmatic membrane, short and thick prolongations were observed (Fig. 4e,f). Type IV_{TEM}, the nucleus presented a marked heterochromatic content and mainly affected the perinuclear zone and extended throughout the nucleus, leaving some zones with euchromatic content. (this section is unclear and requires revision) The contour of the nucleus was irregular, although elongated and thin, like the spindle shape of the cells. The cytoplasmic content was scarce as there were large dilations of the endoplasmic reticulum that occupied a large part of the cytoplasm and some mitochondria. These dilations could merge together and had a content like that of the extracellular matrix. In this cell type it was common to find areas of a material with higher electron density inside. (Fig. 4g,h). Type V_{TEM}, cells with irregular nuclei with heterochromatic content were limited to the perinuclear zone. Occasionally a nucleolus could be observed. They had a cytoplasm containing numerous organelles, such as small electron-dense mitochondria and numerous vesicles of different sizes and electron densities. Some of these vesicles even contained smaller ones inside. In turn, RER could also be observed distributed throughout the cytoplasm. The membrane of these cells had long extensions distributed over the entire surface. According to the already known descriptions, they were identified as Hofbauer cells (Fig. 4i,j).

Inside the dilated endoplasmic reticulum, especially

Table 1. Immunopositivity found in the cytoplasm of mesenchymal cells (type I, II and III) for the different types of proteins studied: growth factors, proteins related to the extracellular matrix, intermediate filament vimentin and microfilament α-actin of the cytoskeleton, connexin 43 component of gap-type intercellular junctions.

Growth factors	Type I	Type II	Type III
VGEF	+/-	++	++/+++
TGF-β2	++/-	+++/++	+++
PDGF-C	-/+	++/+	++/+
FGF-2	+/-	++/+++	+++/++
TGF-β1	-	-	-
FLG	-	-	-
IGF-1	-	-	-
Proteins related with extracellular matrix			
Fibronectin	+	++	++/+++
HSP-47	-	-/±	-/+
Laminin β2	-	-	-
Cytoskeleton			
Vimentin	+	++/+++	+++
α-Actin	±/-	+/-	++/-
Gap junctions			
Connexin 43	+	++/+++	+++

Staining intensity: - negative; ± weakly positive and sometimes negative; + moderately strong; ++ strong; +++ very strong. The / indicates that there are cells with different staining intensity.

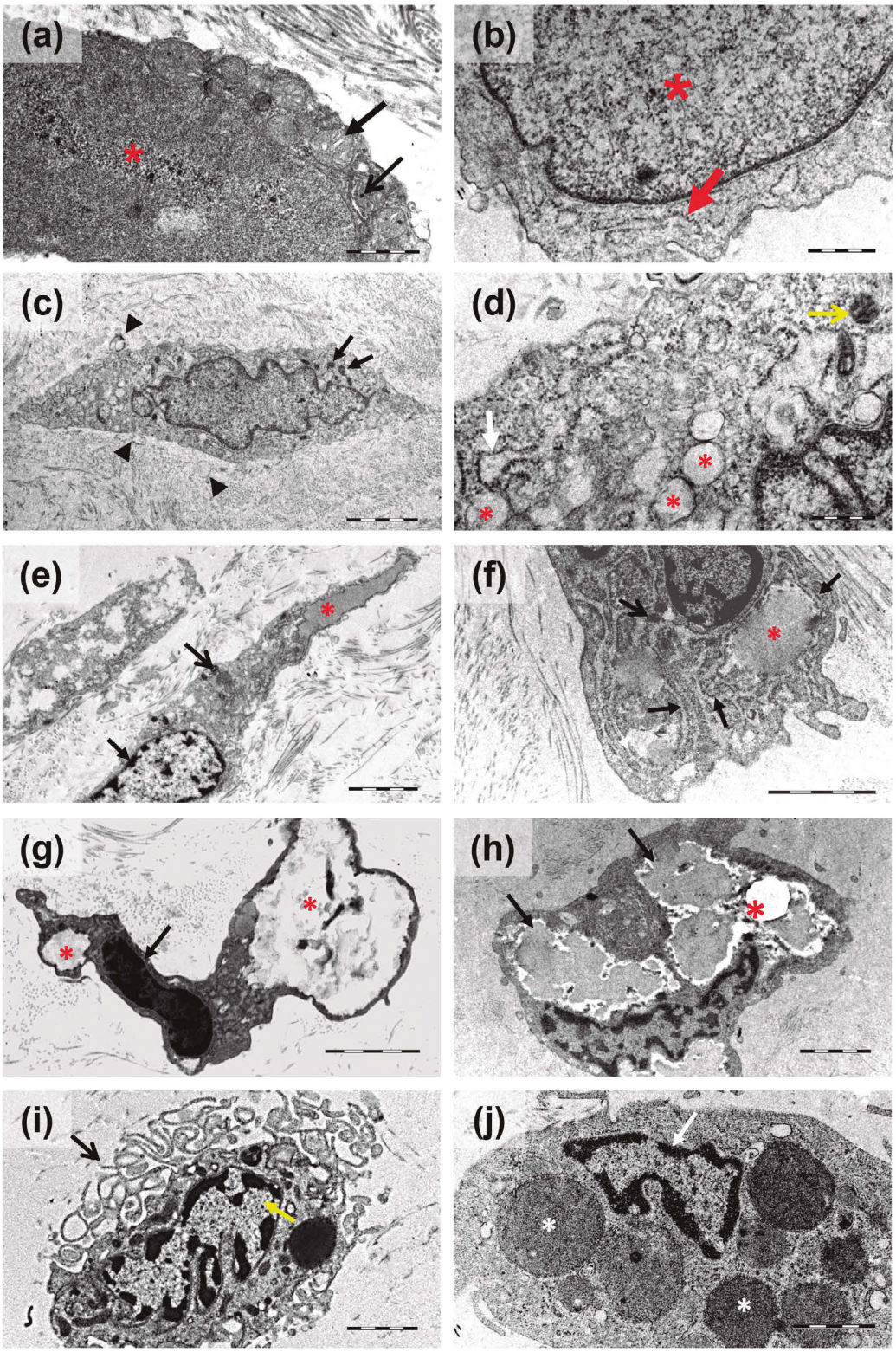

Fig. 4. Characterization by electron microscopy of the different types of mesenchymal cells in the hAM. **a, b.** Type I_{TEM} cells. **a.** Euchromatic nucleus (asterisk) and scant cytoplasm with large mitochondria (arrow) with presence of dense granules (open-headed arrow). **b.** A poorly developed RER is observed in the cytoplasm (arrow) and an euchromatic nucleus (asterisk) is observed. **c, d.** Type II_{TEM} cells: **c.** type II_{TEM} cell with a spindle-shaped morphology and irregularly contoured nucleus, indentations and euchromatic content. The cytoplasm arranged around it is more abundant than in type I_{TEM} and inside there are numerous electron-dense mitochondria (arrows); around the cell diverse vesicles are observed (arrowheads). **d.** A detail of image C, in which the small and electron-dense mitochondria (open-headed arrow) are observed, the developed RER (arrow) that even begins to form vesicular accumulations. The presence of numerous vesicles (asterisks) of homogeneous density stands out from the density of the matrix. **e, f.** Type III_{TEM} cells. Yellow open-headed arrow: mitochondria. **e.** The nucleus with perinuclear heterochromatin (arrow) and mitochondria are observed (open-headed arrow) Dilated RER with material inside (asterisk). **f.** The RER is developed (arrows) and presents large dilations of electron-dense content (asterisk) with globular form preferentially in proximity to the plasma membrane and some small electron-dense mitochondria (open-headed arrow). **g, h.** Type IV_{TEM} cells. **g.** Cell with a very hyperchromatic nucleus, condensed and of reduced size (arrow), the cytoplasm is occupied by dilations (asterisks), one of them large. **h.** The cytoplasm is occupied by dilated RER. The confluence of cisternae is also observed (asterisk). Inside the cisternae a homogeneous material similar in electrodensity to extracellular matrix is observed (arrows). **i, j.** Hofbauer cells. **i.** Cell with very irregular nucleus with large indentations and heterochromatin (arrow). The boundaries of the cytoplasm form long prolongations of plasma membrane (open arrow). **j.** The nucleus is partially observed with perinuclear heterochromatin and irregular contour (arrow) and the cytoplasm shows large lysosomes of different densities (asterisks). Scale bar: a, j, 1 μm; b, d, 0.5 μm; c, e-i, 2 μm.

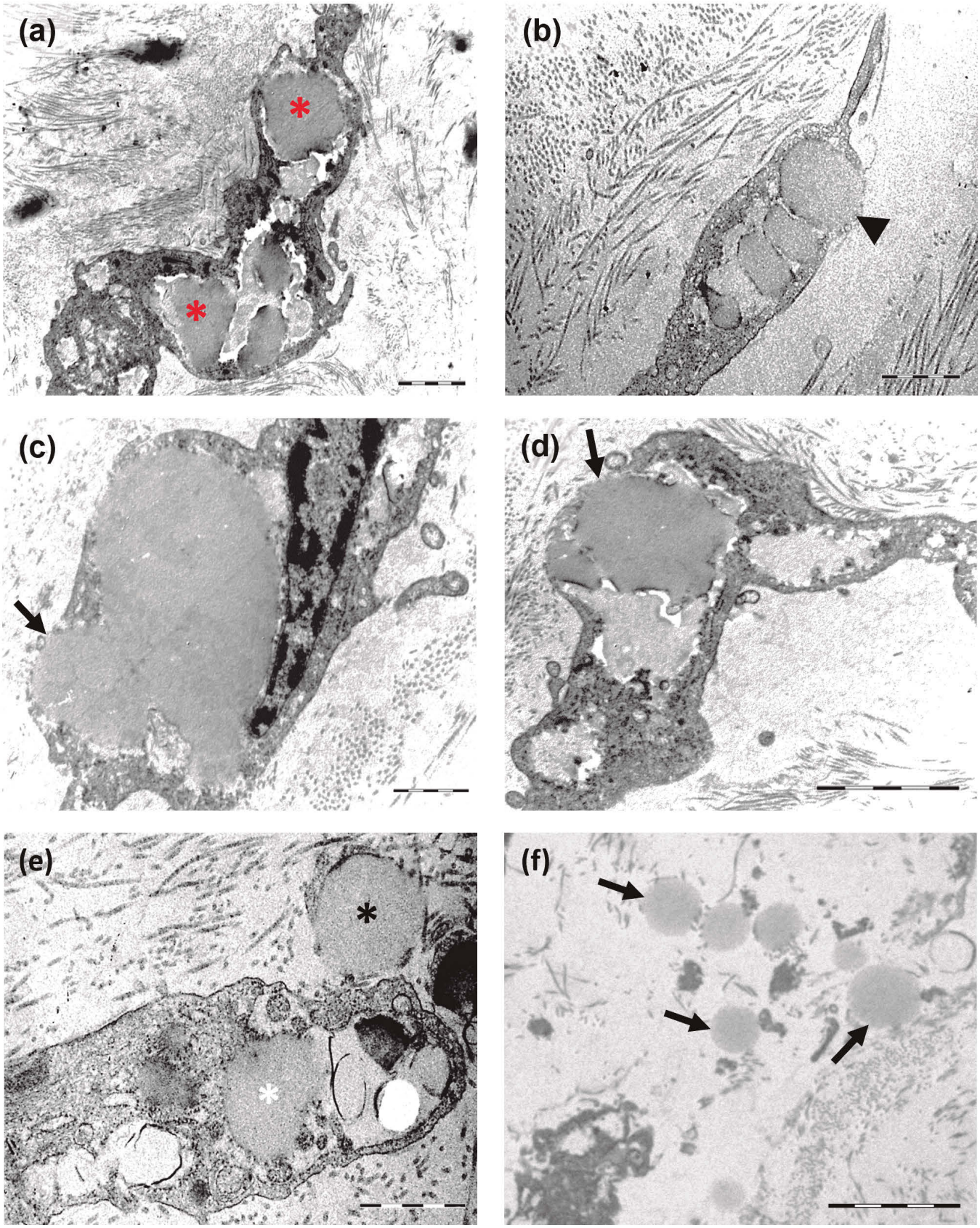

Fig. 5. Electron microscopy of Type III_{TEM} and IV_{TEM} cells in hAM. **a.** Globular material was found in the dilated rough endoplasmic reticulum (asterisk). **b.** This globular material is observed close to the plasma membrane (arrowhead). **c.** In a mesenchymal cell the material is observed in contiguity with the extracellular matrix (arrow). **d.** In another mesenchymal cell, the same phenomenon of apparent secretion from the same RER is observed (arrow). **e.** An extracellular globular material very close to a mesenchymal cell (black asterisk) is observed. In this cell a similar material in the RER (white asterisk) can also be seen. **f.** Diverse presence of globular dense material (arrows) in hAM extracellular matrix. In some cases, they are found close to each other. Scale bars: a, 2 µm; b-d, 1 µm; f, 2.5 µm.

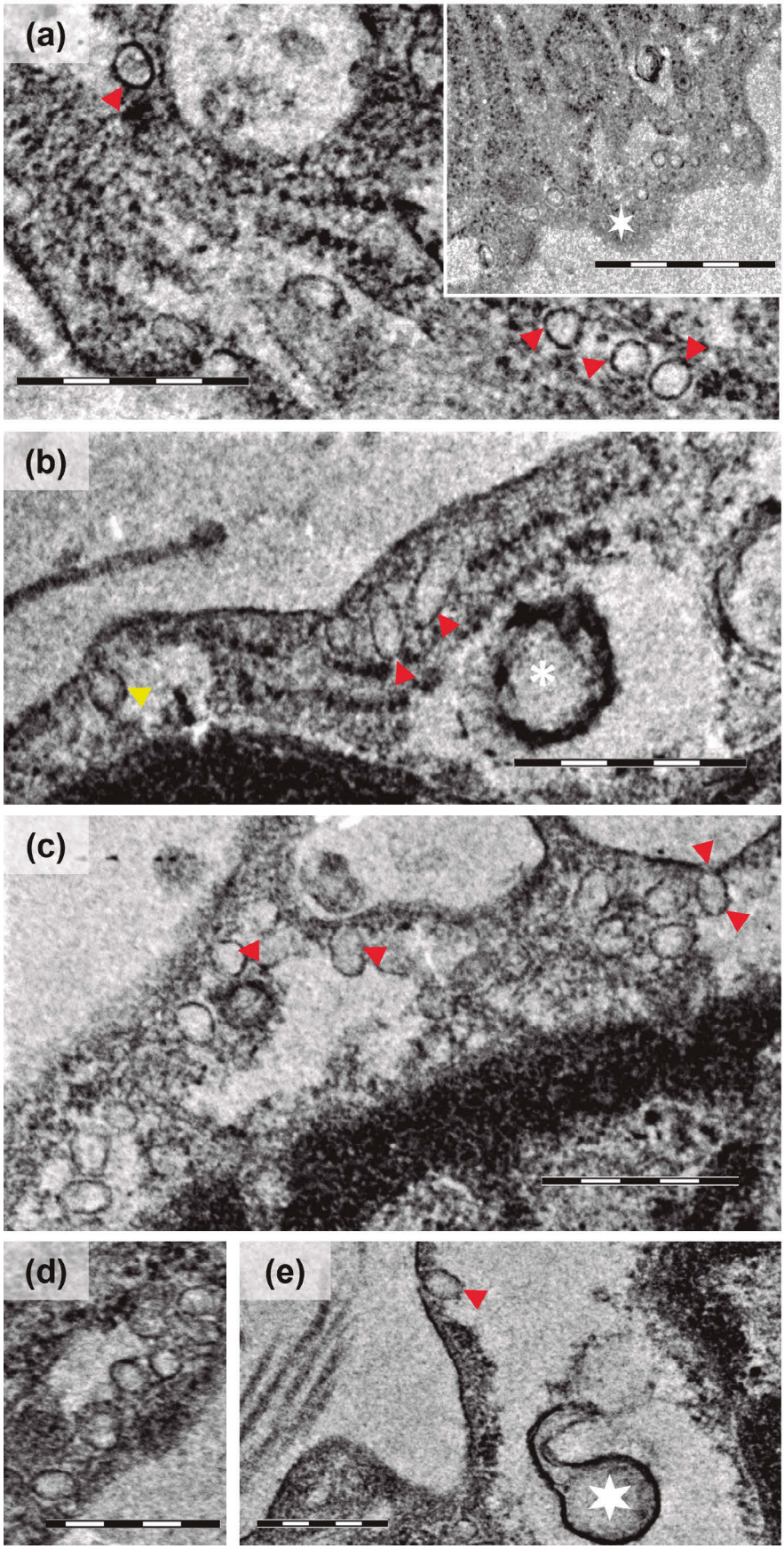

Fig. 6. Vesiculation and possible exocytosis of RER observed using TEM in hAM mesenchymal cells. **a.** Type II_{TEM} cells. Vesiculation of small RER cisterns showing some ribosomes (red arrowheads) is observed in the cytoplasm. Insert: many of them are observed near the plasma membrane (asterisk). **b.** Type III_{TEM} cell. At higher magnification the vesiculation of the RER with material inside (red arrowheads) and its exocytosis (yellow arrowhead) is better observed. Inside the RER cistern there is accumulated material that has trapped another cistern containing material (white asterisk). Type III_{TEM}. **c, d.** Examples of exocytosis of RER vesicles are seen (red arrowheads). **e.** Type IV_{TEM} cell. A large vesicle (asterisk) is seen trapped within a cistern filled with a proteinaceous material. The vesicle has a very electron-dense membrane, probably derived from the ribosomes associated with it. Exocytosis of RER vesicles (red arrowhead). Scale bars: a-e, 0,5 µm; insert a, 1 µm.

of type III_{TEM} and IV_{TEM} cells, the material accumulated in it was observed to form globular structures with higher electron density, approximately 1.5 to 4 µm in diameter, as described above (Fig. 5a,b). Also, within the matrix inside the reticulum, globular structures of smaller diameter and with 0.4-0.8µm electron-dense edges were observed (Fig. 5e). In addition, on several occasions we could see how the reticulum cisterns contacted the plasma membrane, producing a continuity between the interior of the reticulum with the nearby extracellular matrix, suggesting a release of the globular structures contained within (Fig. 5b-d). In the vicinity of the cells, these structures were found with the same electron density and sizes (Fig. 5e,f). Together with these structures, some smaller ones that presented an electron-dense edge were also observed and were probably also derived from the interior of the reticulum (Fig. 6a-e). At higher magnification, it was observed that especially in type II_{TEM} and III_{TEM} cells the RER suffered vesiculation, although it was also observed in IV_{TEM} cells to a lesser extent. Vesicles of 0.1 to 0.2 µm had a small electrolucent content inside and were observed in the vicinity of the plasmatic membranes, many of them were in a process of probable exocytosis (Fig. 6c).

Light microscopy semiquantitative study of mesenchymal cell types

The different types of mesenchymal cells described above, as well as Hofbauer cells (Type IV), were observed in all sections analyzed. After the counts were performed and their percentage calculated, the mean index of each of the cell types with respect to the total population of cells counted from the fibroblastic layer of the amniotic membrane of the periumbilical area studied was obtained. The mean percentage index of type I cells (1.77±0.68) was significantly lower ($p<0.05$) compared to the index of type II cells (58.43±6.47) and type III cells (32.29±5.35), but not with that of type IV cells (7.49±2.16). The mean percentage rate of type II cells was significantly higher ($p<0.05$) than that of types I, III and IV. The index of type III cells was significantly higher ($p<0.05$) with respect to the index of type I and IV. Finally, the percentage rate of type IV cells was significant ($p<0.05$) with the rates of type II and III cells, but not with that of type I cells (Fig. 7).

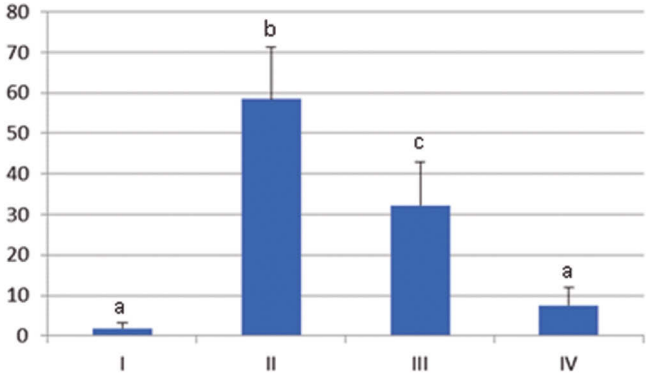

Fig. 7. Percentage index of each of the mesenchymal cell types found: I, II, III, IV. a, b, c indicates significant differences between the percentage index of observed mesenchymal cell types ($p<0.005$).

Semiquantitative study with transmission electron microscopy

The study of the mesenchymal cell population showed the existence of heterogeneity in terms of their distribution ($p<0.0001$). Thus, it was possible to distinguish three groups of cells: a) a low abundance group that included types I and II, b) another group of very abundant cells that corresponded only to type $II_{TEM}I$ cells, and c) a group of cells that included types III_{TEM}, IV_{TEM} and V_{TEM}. The grouping of type III_{TEM} cells was relatively larger compared to the other cell groups, whereas the group of type I_{TEM} and II_{TEM} cells was relatively smaller compared to the other two groups (Table 2).

Discussion

Diverse types of mesenchymal cells are identified with light microscopy

The hAMs in our study already have their tissue structure described (Bourne, 1960, 1962, 1966; Bachmaier and Graf, 1999; AL-Yahya and Makhlouf, 2013). The fibroblastic layer was usually formed by more than one row of cells, where it was easy to distinguish the presence of three types of mesenchymal cells. With semithin sections, four cell types were differentiated, one of them being Hofbauer cells, which were frequently observed in contact with mesenchymal cells. Semiquantitatively, the percentage of each of the cells showed that type II cells were the most frequent, followed by type III cells, which were more frequent than type I and IV but less than type II cells. No statistically significant differences were found between type I and IV.

The morphological heterogeneity of amniotic

Table 2. Mesenchymal cell $types_{TEM}$ (A) and their frequency found after analysis of the grids studied (B). After statistical analysis, the residuals (C) were obtained, which showed that the groupings were significant.

A Cell $Types_{TEM}$	B Frequency	C Residuals
I (a)	3	-3.79
II (a)	6	-2.98
III (b)	38	5.69
IV (c)	15	-0.54
V (c)	23	1.63

Type I and II <2 and type 3>2 cells.

mesenchymal cells has been proposed on some occasions, but exclusively after their isolation and culture "*in vitro*". In these works, reference is made to two cell types, one with polygonal or rounded morphology and the other with spindle-shaped morphology, without going into more cellular details. Furthermore, this heterogeneity may be partially or totally exacerbated by the contamination of epithelial cells that have been co-cultured with mesenchymal cells when these are obtained from the amniotic membrane. In other studies, heterogeneity is not observed, for example, in cultures of mesenchymal cells from chorionic villus and umbilical cord, where isolation of mesenchymal cells is easier (Mihu et al., 2009; Bačenková et al., 2011; Barbati et al., 2012; Shaer et al., 2014; Rylova et al., 2015; Araújo et al., 2017). Whether or not there is mesenchymal heterogeneity, the cell population in culture progressively evolves towards morphological homogenization with each culture passage, until authentic fibroblastic homogeneity is reached. *In vitro*, then, it is suggested that epithelial cells themselves become mesenchymal cells, the so called epithelial-mesenchymal transition, as if there were a true fibroblastic differentiation of initially heterogeneous mesenchymal cells (Mihu et al., 2009; Bačenková et al., 2011; Shaer et al., 2014; Vellasamy, 2012; Rylova et al., 2015; Araújo et al., 2017). On the contrary, the ease of isolating mesenchymal cells from the umbilical cord, unlike the amniotic case, has traditionally described cell homogeneous cultures (Mihu et al., 2009; Bačenková et al., 2011; Barbati et al., 2012; Shaer et al., 2014; Rylova et al., 2015; Araújo et al., 2017). Other authors have described heterogeneity between umbilical cord mesenchymal cells, describing two sets of subpopulations based on cell size, small cells, with higher nucleus-cytoplasm ratio, higher proliferative capacity and higher expression of stem cell markers, and another set of large cells, more abundant than the previous one, with lower expression of stem cell markers, lower proliferative activity, and higher presence of senescent cells (Majore et al., 2009). Regarding "*in vivo*" studies, there are no descriptions of mesenchymal cells at the end of pregnancy in the amniotic membrane. Our results suggest that a diverse population of mesenchymal cells exists at this time. Based on the morphology they present, we can identify a cell population, type I, which is scarce in proportion to the other types, and morphologically very similar to stem cells found and described in other tissues, especially in mouse, primate, and human mesenchymal tissues (van Bekkum et al., 1971; Tumbar et al., 2004; Vestentoft, 2013). The type II and III cell population show morphological characteristics of fibroblastic cells (Eyden, 2004), with the peculiarity of presenting significant dilations in their cytoplasm in which numerous globular deposits of toluidine-positive material are observed that do not stain with H&E. From all these observations we can conclude the presence of morphologically different types of mesenchymal cells in the amniotic membranes studied, which probably represent stages of lower to higher fibroblastic differentiation of these cells.

Collagen, mainly type I and III, has traditionally been described as the main component of the extracellular matrix, which gives the tissue most of its biomechanical characteristics. Collagen IV remains the most representative of the basal membrane, with laminin (Bryant-Greenwood, 1998; Malak et al., 1993) and fibronectin in the compact layer (Ockleford et al., 1993). Proteoglycans and hyaluronic acid and other proteins such as fibronectin are found in hAM (Meinert et al., 2001). Our observations with PAS staining agree with those of other authors showing both the basement membrane as the compact layer zone with abundant type III collagen fibers, and fibronectin produced by amniotic cells (Alitalo et al., 1980; Aplin et al., 1985; Strauss, 2013). The positivity found for Alcian blue with both types of pH is related to the presence of anionic groups throughout the extracellular matrix studied. Sulfate or carboxylated anions in the amniotic membrane have been especially related to the presence of proteoglycans and hyaluronic acid. The latter has been localized especially in the spongy layer where it can create a high swelling pressure of the tissue because of its high-water binding capacity that enables separate the amnion and chorion. This property acts as a gliding layer during the birthing process and thus protect the fetus (Meinert et al., 2001). The presence of sulfate groups revealed in our work by Alcian Blue at pH 1 in the compact and spongy areas is probably related to decorin, biglycan or lumican. These are proteoglycans containing chondroitin, keratan or dermatan sulfate (Iozzo and Schaefer, 2015). Finally, it should be noted that the images obtained did not show positivity for both Alcian dyes in the cytoplasm of mesenchymal cells, which could indicate an interruption in the passage of these proteins from the RER to the Golgi apparatus. Something that contrasts with the positivity to PAS in the cytoplasm of mesenchymal cells that increases from type I to III cells and might imply that the glycosylation process stops early, when the oligosaccharides bound to these proteins still present mannose and glucose inside the reticulum (Li et al., 2012; Mikami and Kitagawa, 2013). The positivity to Concanavalin-A lectin specific for mannose or glucose residues (Pinart et al., 2001) suggests that there is a progressive accumulation of these proteins in the reticulum of the mesenchymal cells.

Immunohistochemical study shows a pattern of fibroblastic differentiation in mesenchymal cell types

The various proteins that have been identified immunohistochemically in hAM have been located in mesenchymal cells, except for fibronectin, which has also been identified in the compact layer. Two important facts should be highlighted, on the one hand, that immunopositivity has been increasing in intensity from type I to type III cells for all types of proteins detected.

On the other hand, the positivity for fibronectin is observed in the cytoplasm distributed irregularly and in intracytoplasmic globular structures with strong positivity. Fibronectin is an extracellular matrix glycoprotein, in humans there are at least two isoforms of fibronectin, human plasmatic fibronectin and fetal fibronectin, which differ from each other mainly in protein glycosylation. Its main function in the amniotic membrane is support, thanks to its great binding capacity to surface receptors, collagen, proteoglycans, and other fibronectin molecules (Zhu et al., 1984; Köttgen et al., 1989; Mogami et al., 2013). Synthesis peaks in the early stages of pregnancy, during the first trimester, and gradually decreases to become minimal between weeks 25-36, and then undergoes a significant increase again in the last weeks before delivery. This has made it possible to relate the amount of fibronectin released from the fetal membranes to vaginal fluid as a marker of preterm labor and even of chronologically prolonged gestations (Lockwood et al., 1991, 1994). The fibronectin was also observed in hAM especially in the compact layer by other authors (Ockleford et al., 1993) and is considered to be responsible for mechanical strength in the amniotic membrane (Bourne and Lacy, 1960). The results obtained with immunohistochemical staining of fibronectin in our study correlate with those observed for PAS and Concanavalin-A since fibronectin in its glycosylation presents mannose residues and the carbohydrate portion of fibronectin is synthesized as a 'high-mannose' intermediate and subsequently processed to give the 'complex' oligosaccharide chains characteristic of this protein (Olden et al, 1980). In addition, one of the most interesting aspects observed is the increased positivity in type III cells compared to type I cells and the formation of globular bodies distributed throughout the cytoplasm and presenting a distribution like that found with the Concanavalin A and PAS, as previously indicated. Moreover, this positive distribution of cells was also observed in the semithin sections. These facts seem to show an arrest of fibronectin in the endoplasmic reticulum, as well as the possible release of fibronectin in the form of globular structures in the extracellular matrix. This fact further reaffirms the process of fibroblastic differentiation of mesenchymal cells that occurs between type I and III cells to the extent that fibronectin synthesis is typical of fibroblast cells or myofibroblasts (Kaarteenaho-Wiik et al., 2009; Moretti et al., 2022).

In this study, various growth factors have been found in the mesenchymal cells of the hAM. VEGF has been proposed as an important regulator of amniotic fluid absorption through the amnion into the fetal vasculature on the placental surface (Cheung et al., 2014, 2019). Thus, although the amniotic epithelium and cytotrophoblast have traditionally been described as the main source of VEGF (Clark et al., 1996; Bogic et al., 2000), in our work we have been able to identify positive amniotic mesenchymal cells, as has been observed in culture of hAM mesenchymal cells (Dabrowski et al., 2017) suggesting that the increase of VEGF in the final stages of pregnancy, a fact described by other authors (Bogic et al., 2000) could also be related to a relative increase of type III cells at the end of gestation. Expression of TGF-β 1, 2 and 3 in the cytotrophoblast, decidua and epithelium of hAM have been found in amniotic membrane with various methods (Graham et al., 1992; Lysiak et al., 1995; Schilling and Yeh, 2000, Koizumi et al., 2000; Grzywocz et al., 2014) but there were doubts about the expression of TGF-β2 in mesenchymal cells, since there are no specific results so far about the expression of this factor in these cells, something that is found in our work. PDGF-C in the placenta has traditionally been related to its angiogenic function, important for the maturation of blood vessels, although its presence has not been determined so far in mesenchymal cells "*in vivo*" (Li et al., 2000; Cao et al., 2002; Tian et al., 2019). PDGF-C appears to play an important role in the initial differentiation of fibroblasts and in the appearance of the recently named proto-myofibroblasts, a population of fibroblasts activated from tissue-resident fibroblasts (Tomasek et al., 2002). FGF-2 or bFGF is part of the family of heparin-associated growth factors and is involved in numerous essential biological aspects such as embryonic development, tissue repair, cardiovascular disease, angiogenesis, neuronal survival or cancer (Hui et al., 2018). In hAM bFGF has been found by the ELISA method (Bischoff et al., 2017) and qRT-PCR results revealed that crucial angiogenic genes that are beneficial for vascular regeneration, such as VEGF-A, Ang-1, HGF, and FGF-2, that are highly found in hAMSCs (Kim et al., 2012). To date, a comprehensive immunohistochemical study of FGF-2 in hAMSCs has not been performed. All these growth factors, among others, have been found in the extracellular matrix of the hAM and confer regenerative properties that have been used in a wide variety of pathological processes, as their use is associated with faster and more functional tissue recovery (Liu et al., 2020; Lo and Pope, 2009; Strueby and Thébaud, 2016; Tang et al., 2018). Although both epithelial and mesenchymal cells are known to contribute to the synthesis and release of these factors, they have not always been identified "*in vivo*", and the exact role they play in fetal membranes at term is unknown. In our study, the factors studied in general show higher positivity in their cytoplasm when the cell acquires a more fibroblastic morphology, i.e., in type III cells. These results also indicate the importance of the mesenchymal cells themselves in the synthesis and release of these factors.

Vimentin is a type III intermediate filament associated with mesenchymal cells, or the epithelial-mesenchymal transition, related to cell motility, cell adhesion to the extracellular matrix, and collagen deposition (Paulin et al., 2022). Its absence, on the contrary, is associated with a loss of cell morphology and defective fibroblastic directional migration. Vimentin is distributed dispersed throughout the

cytoplasm of fibroblast cells (Ostrowska-Podhorodecka et al., 2022) and participates in the morphological configuration of the cells, there being a directly proportional relationship between the amount of cytoplasmic vimentin and the fibroblastic morphology of the cell (Mendez et al., 2010). According to the above, type III cells, which show greater positivity to vimentin, would have a more fibroblastic phenotypic character. The observed heterogeneity of mesenchymal cells would be related to a progressive acquisition from I to II of these cell phenotypes, something that would also be related to the positivity of HSP-47 and α-actin. But along with this are signs that type III cells are not fully active fibroblasts. The low cytoplasmic positivity of HSP-47 and the fact that many of the cells are not α-actin positive, something already observed in other studies (McParland et al., 2000), together with the probable dilation of the RER, might be related to defective protein aggregation. This would mean that protein synthesis, especially in type III cells, would be blocked or, if a part of them is released, they would probably be defective, affecting the integrity of the extracellular matrix. In summary, the possible mesenchymal differentiation observed from type I to type III cells in this study would lead to a more fibroblastic cell type with dysfunctional character for these cells.

The ultrastructure of mesenchymal cells allows to describe four types of these cells

The ultrastructural characterization carried out has not only allowed us to identify the types of mesenchymal cells observed with light microscopy, but also to observe a possible transition between them, having differentiated a new cell type that would be inserted between types II and III observed with light microscopy. Together with this, the organelles of the different cells showed a gradual complexity from type I_{TEM} to type IV_{TEM}. It is noteworthy the great development occurring in the RER that affects both its dilation, occupying a large part of the cytoplasm, and the increase in its interior of a material with a texture very similar to that observed in the surrounding extracellular matrix. Finally, it was possible to easily identify the Hofbauer cells. The semiquantitative determination of the population of these cells indicates that the periumbilical membrane studied presents a heterogeneity of mesenchymal cells, with type III_{TEM} being significantly the most abundant.

The results found in cells I-IV_{TEM} show changes partially compatible with fibroblastic differentiation described by other authors in fibroblasts (Han et al., 1965), in human chorionic villus fibroblasts (Jones and Fox, 1991) or the umbilical cord (Takechi et al., 1993) but do not show certain ultrastructural characteristics typical of fibroblast or myofibroblast (Eyden, 2004). In hAM the few ultrastructural descriptions of mesenchymal cells encompass them all in a group of undifferentiated cells and consider that the RER dilations observed by us are probably lipid deposits (Al-Yahya and Makhlouf, 2013). Therefore, in the various ultrastructural studies on the hAM, we have could not find any description about the existence of different types of mesenchymal cells. Regarding each of the mesenchymal cell types found in our study, we consider that type I_{TEM} cells are similar to those of mesenchymal stem cells derived from human amnion (Pasquinelli et al., 2007), and even to mesenchymal stem cells derived from other tissues such as rat, horse or sheep bone marrow (Karaoz et al., 2009; Paul et al., 2012), although it should be noted that all the mesenchymal cells mentioned have been described "*in vitro*". We believe that the greater or lesser presence of this mesenchymal type within the amniotic membrane should be taken into account when obtaining amniotic membrane for the procurement of mesenchymal cells in regenerative medicine. As for type II_{TEM}, they are like those observed in the early stages of embryonic development of the amniotic membrane. They develop an important synthetic activity that is fundamental in the formation of the extracellular matrix of the fetal amniotic membrane (Jones and Jauniaux, 1995). Similar fibroblastic differentiation data have also been observed in amniotic membranes of different gestational ages (Hoyes, 1970), with cells similar to type II_{TEM} being observed in the younger membranes, and like type III_{TEM} in the membranes of longer gestational time. Along with this, some similar cells to type II_{TEM} and III_{TEM} have also been observed in human chorionic villi. They describe "fibroblasts" with a dilated endoplasmic reticulum, numerous secretion vesicles, and the Golgi apparatus (Jones and Fox, 1991). Our observations seem to indicate that the cell types found in this study are related to a progressive differentiation process, in which type I_{TEM} is the most immature cell, type II_{TEM} and III_{TEM} cells are those with the highest synthetic activity, while type IV_{TEM} constitutes a cell at its maximum differentiation stage, or even in a senescent stage, as the cell organelles decrease or express β-galactosidase activity (Han et al., 1965; Gomez-Lopez et al., 2017). Both in the chorionic villi and the fibroblast population described in the umbilical cord (Takechi et al., 1993) there do not appear to be cells morphologically similar to the type IV_{TEM} cells observed in our work. One explanation for the fact that the joint presence of several types of hAM mesenchymal cells (fibroblasts) was not observed in other previous studies could be related to the location in which these cells reside. Thus, it is logical to assume that the chorionic villi or umbilical cord are essential throughout fetal development until moments before delivery and that fully active mesenchymal cells are required. The fact that we found these type IV_{TEM} cells in our study, but in a lower proportion than type III_{TEM} cells, could be due to the fact that the samples studied in this hAM work belong to the periumbilical portion which, although it undergoes some stress during childbirth, is not comparable to that found in other

locations of the hAM such as the area of rupture or the hAM of the uterine wall. It is possible that in these areas there is a greater abundance of type IV_{TEM} mesenchymal cells than in the periumbilical area, especially in eutocic deliveries, something that will have to be verified in subsequent studies.

The material included in the dilated RER presented a morphology similar to that surrounding extracellular matrix

One of the most characteristic findings of the mesenchymal cells studied was the observation of a highly dilated RER that contained a material similar to that of the extracellular matrix and with homogeneous globular structures inside. It is known that RER dilation may be associated with a dysfunctional process of protein synthesis, the origin of which may be due to a variety of causes (Liong and Lappas, 2014; Veerbeek et al., 2015). Abnormally configured proteins often accumulate inside the reticulum, including collagen fibers altered by the absence of HSP-47. In several observations of placental tissues these RER dilations have traditionally been described in relation to oxidative stress (Malhotra and Kaufman, 2007; Yung et al., 2008; Veerbeek et al., 2015). Although the hAM is also affected by oxidative stress at the molecular and histological level (Liong and Lappas, 2014), there is only electron microscopy data for other placental tissues. Moreover, a direct link has been established between RER stress and placental insufficiency, with defective folding of proteins in RER, and with altered protein glycosylation (Yung et al., 2008). Usually, in cells, the production of abnormally configured proteins leads to an interruption of their release into the Golgi apparatus and their accumulation in the RER with its secondary dilation (Ishida et al., 2006; Veerbeek et al., 2015). These abnormal proteins are able to assemble inside the RER, forming compact amorphous, protofibrillar, or circular morphology deposits that trigger a signaling cascade known as unfolded protein response (UPR) (Ishida et al., 2006; Malhotra and Kaufman, 2007; Lindquist and Kelly, 2011; Kim et al., 2013; Pluquet et al., 2015). If this regulatory response -proteostasis- fails to restore functional protein production, RER stress ultimately leads to a decrease in cell cycle regulatory proteins, associated with a decrease in cell proliferation, and even when stress is very high, cell apoptosis or senescence. All of this is related to the continuous increase in the deposit of misfolded proteins in the RER (Malhotra and Kaufman, 2007; Yung et al., 2008, Liong and Lappas, 2014; Pluquet et al., 2015; Druelle et al., 2016; Lyublinskaya et al., 2021). Likewise, molecular activation triggered by RER stress has been linked to an increase in senescence-associated secretory phenotypes (SASP) molecules with a proinflammatory profile, that may be behind numerous diseases, also affecting mesenchymal cells (Malhotra and Kaufman, 2007; Liong and Lappas, 2014; Pluquet et al., 2015; Tavasolian et al., 2020; Lin and Xu, 2020; Liu et al., 2020). In SASP cells, bFGF, fibronectin VEGF, TGFβ or matrix metalloproteinases are more highly expressed and secreted into the surrounding medium (Coppé et al., 2010; Liu et al., 2020). Related to the above, studies on fetal membranes have shown that placentas that have undergone the birth process in a normal and spontaneous manner, compared to term fetal membranes that have not undergone this process, have higher levels of molecules associated with labor stress (IRE1, GRP78 or XBP1) (Liong and Lappas, 2014; Veerbeek et al., 2015). Higher levels of these proteins are also associated with higher levels of proinflammatory molecules (Liong and Lappas, 2014), even describing the RER dilation as the clearest visual sign of RER stress, present in syncytiotrophoblast cells. Finally, it should be noted that Liong and Lappas (2014) show that the increase in UPR proteins, in RER stress, begins rapidly, both in term and preterm placentas, in relation to the birth process. In summary, based on the above, we could consider that there seems to be a fibroblastic differentiation process of mesenchymal cells that is gradual and whose term seems to correspond to type III_{TEM} and IV_{TEM} cells. This process has been found in mesenchymal cells of hAM that have not suffered the effects of the birth process, as they came from cesarean sections, which indicates, on the one hand, that it is a starting phenomenon probably linked to gestational age. On the other hand, it raises the possibility that in the amniotic membranes that undergo the birth process, the percentage of type III_{TEM} and IV_{TEM} cells may be increased, since this process produces a high oxidative stress that could lead to an accelerated maturation of these cells, increasing the percentages of them in said membranes.

Possible direct secretion from the RER into the extracellular matrix

To complete the above, we have ultrastructurally observed in our study, first of all, a striking fact that we believe has not been described in the literature; the capacity of type III_{TEM} but especially of type IV_{TEM} cells, to release glycoprotein aggregates accumulated in the endoplasmic reticulum into the extracellular matrix. These can be found in the vicinity of the mesenchymal cells. Observations like these, though not described, have been seen in the extracellular matrix in human Wharton's jelly (Takechi et al., 1993) or large amounts of amorphous material are observed in the spongy layer (Bou-Resli et al., 1981; Ibrahim et al., 1983). Regarding the way in which the contents of the dilated RER are released, in our study it has been observed that this occurs by fusion with the plasma membrane, being a peculiar phenomenon that has rarely been described in the literature. Thus, the possibility that this form of secretion exists in skin fibroblasts has been considered for years (Ross and Benditt, 1965; Ross, 1975). Nowadays, several authors speak of the existence of unconventional secretory mechanisms of cells without

the intervention of the Golgi apparatus (Nickel and Rabouille, 2009) but the molecules that have been shown to be secreted directly from the ER are not from the extracellular matrix. Given that the electron microscopy images coincide with the structures which, with light microscopy, showed a high mannose and fibronectin content, we believe that a high percentage of the content accumulated in the reticulum and later released belongs to this important extracellular matrix protein, which is usually processed in its final phase in the Golgi apparatus (Olden et al., 1980). In various experimental or pathological situations, accumulation of fibronectin in the ER has been described, as well as abnormal deposition in the extracellular matrix of this protein, which can form amyloid-like structuration (Ledger et al., 1980; Vitellaro-Zuccarello et al., 1989; Papp et al., 2007; Yoshino et al., 2007; Kii et al., 2016; Takii et al., 2017; Bascetin et al., 2018; Mezzenga and Mitsi, 2019). Defective fibronectin would indicate the dysfunctional character of type III_{TEM} and IV_{TEM} cells. In addition, since these cells are highly positive for various growth factors, they could present a senescent phenotype (SASP), involved in the clean inflammatory response and in the degradation of the extracellular matrix of the fetal membranes in what is called the physiologic inflammatory process (Menon et al., 2020). Bearing in mind that our observations have been made with hAM without labor, we can think that membranes that undergo labor with the consequent increase in oxidative stress should show an increase in these secretions that we are discussing and that would be linked to a possible increase in percentage of Type III_{TEM} and IV_{TEM} mesenchymal cells. This could be related to the degradation processes of the extracellular matrix associated with the rupture of fetal membranes during childbirth. Specific studies are needed to verify these hypotheses. Lastly, Hofbauer cells, which in our study we have called Type V_{TEM} cells in electron microscopy, are frequent in fetal membranes and in placental trunks and villi. In the hAM they can be found distributed throughout the amniotic fibroblastic layer with typical macrophage morphology with numerous intracytoplasmic vacuoles of different electron density, related to lysosomal/phagocytic bodies in different states of digestion derived from phagocytosis of the extracellular matrix (Enders and King, 1970).

Conclusion

In conclusion, the mesenchymal cells of the fibroblastic layer of the amniotic membrane studied are not a homogeneous population. Different cell types have been found that seem to indicate a transition from poorly differentiated cells to fibroblastic cells that are probably senescent. This transition also implies an increase in the expression of growth factors in them, as well as the accumulation of fibronectin protein in their RER. These results may be of interest both for the extraction of mesenchymal stem cells from the hAM for use in regenerative medicine, and for understanding the mechanisms of membrane rupture during childbirth. Both questions require a similar study to that carried out in other locations of the membrane, especially after normal births in which the membrane and the mesenchymal cells it contains have undergone the cellular stress associated with this process.

Acknowledgements. We thank Mrs M.C. Gonzalez Ulloa for laboratory assistance (University of Murcia), and all the members of the Electron Microscopy Service (University of Murcia) for their technical assistance.
Author contributions. Salvador Cortes-Sandoval, Vicente Seco-Rovira and Esther Beltrán-Frutos were involved in the research design, acquisition, analysis, interpretation of data and drafting the paper. Carmen Insausti and Miguel Blanquer participated in the acquisition and interpretation of data. Concepción Ferrer, Jesús Martínez-Hernández, María Isabel Serrano and Juan Luis Delgado participated in the interpretation of data and paper revision. Luis M. Pastor participated in all phases of the drafting of this paper.
Funding. Jesús Martínez-Hernández was financially supported by the Ministry of Universities (Spain) and by European Union-Next Generation EU Funds (Margarita Salas Scheme-181/MSJD/22).
Data availability statement. All original data are available from the authors on request.
Declaration of competing interest. The authors declare no conflicts of interest for this paper.

References

AL-Yahya A.R. and Makhlouf M. (2013). Characterization of the human amniotic membrane: Histological, immunohistochemical and ultrastructural studies. Life Sci. J. 10, 3701-3710.

Alitalo K., Kurkinen M., Vaheri A., Krieg T. and Timpl R. (1980). Extracellular matrix components synthesized by human amniotic epithelial cells in culture. Cell 19, 1053-1062.

Alviano F., Fossati V., Marchionni C., Arpinati M., Bonsi L., Franchina M., Lanzoni G., Cantoni S., Cavallini C., Bianchi F., Tazzari P.L., Pasquinelli G., Foroni L., Ventura C., Grossi A. and Bagnara G.P. (2007). Term amniotic membrane is a high throughput source for multipotent mesenchymal stem cells with the ability to differentiate into endothelial cells *in vitro*. BMC Dev. Biol. 7, 11.

Aplin J.D., Campbell S. and Allen T.D. (1985). The extracellular matrix of human amniotic epithelium: ultrastructure, composition and deposition. J. Cell. Sci. 79, 119-136.

Araújo A.B., Salton G.D., Furlan J.M., Schneider N., Angeli M.H., Laureano Á., Silla L., Passos E.P. and Paz A.H. (2017). Comparison of human mesenchymal stromal cells from four neonatal tissues: Amniotic membrane, chorionic membrane, placental decidua and umbilical cord. Cytotherapy 19, 577-585.

Bachmaier N. and Graf R. (1999). The anchoring zone in the human placental amnion: bunches of oxytalan and collagen connect mesoderm and epithelium. Anat. Embryol. (Berl). 200, 81-90.

Barbati A., Grazia Mameli M., Sidoni A. and Di Renzo G.C. (2012). Amniotic membrane: separation of amniotic mesoderm from amniotic epithelium and isolation of their respective mesenchymal stromal and epithelial cells. Current Protocols in Stem Cell Biology, Chapter 1, Unit 1E.8.

Bascetin R., Blay L., Kellouche S., Carreiras F., Picot C.R., Briand M.,

Agniel R., Gallet O., Vendrely C. and Leroy-Dudal J. (2018). Fibronectin amyloid-like aggregation alters its extracellular matrix incorporation and promotes a single and sparsed cell migration. Exp. Cell Res., 371, 104-121.

Bačenková D., Rosocha J., Tóthová T., Rosocha L. and Šarisský M. (2011). Isolation and basic characterization of human term amnion and chorion mesenchymal stromal cells. Cytotherapy 13, 1047-1056.

Behnia F., Taylor B.D., Woodson M., Kacerovsky M., Hawkins H., Fortunato S.J., Saade G.R. and Menon R. (2015). Chorioamniotic membrane senescence: a signal for parturition? Am. J. Obstet. Gynecol. 213, 359.e1-16.

Bischoff M., Stachon T., Seitz B., Huber M., Zawada M., Langenbucher A. and Szentmáry N. (2017). Growth factor and interleukin concentrations in amniotic membrane-conditioned medium. Curr. Eye Res. 42, 174-180.

Bogic L.V., Brace R.A. and Cheung C.Y. (2000). Cellular localization of vascular endothelial growth factor in ovine placenta and fetal membranes. Placenta 21, 203-209.

Bou-Resli M.N., Al-Zaid N.S. and Ibrahim M.E. (1981). Full-term and prematurely ruptured fetal membranes. An ultrastructural study. Cell Tissue Res. 220, 263-278.

Bourne G.L. (1960). The microscopic anatomy of the human amnion and chorion. Am. J. Obstet. Gynecol. 79, 1070-1073.

Bourne G. (1962). The foetal membranes. A review of the anatomy of normal amnion and chorion and some aspects of their function. Postgrad. Med. J. 38, 193-201.

Bourne G.L. (1966). The anatomy of the human amnion and chorion. Proc. R Soc. Med. 59, 1127-1128.

Bourne G.L. and Lacy D. (1960). Ultra-structure of human amnion and its possible relation to the circulation of amniotic fluid. Nature 186, 952-954.

Bryant-Greenwood G.D. (1998). The extracellular matrix of the human fetal membranes: structure and function. Placenta 19, 1-11.

Calvo A., Pastor L.M., Horn R. and Pallares J. (1995). Histochemical study of glycoconjugates in the epididymis of the hamster (Mesocricetus auratus). Histochem. J. 27, 670-680.

Cao R., Bråkenhielm E., Li X., Pietras K., Widenfalk J., Ostman A., Eriksson U. and Cao Y. (2002). Angiogenesis stimulated by PDGF-CC, a novel member in the PDGF family, involves activation of PDGFR-alphaalpha and -alphabeta receptors. FASEB J. 16, 1575-1583.

Cheung C.Y., Beardall M.K., Anderson D.F. and Brace R.A. (2014). Prostaglandin E2 regulation of amnion cell vascular endothelial growth factor expression: relationship with intramembranous absorption rate in fetal sheep. Am. J. Physiol. Regul. Integr. Comp. Physiol. 307, R354-360.

Cheung C.Y., Anderson D.F., Rouzaire M., Blanchon L., Sapin V. and Brace R.A. (2019). Retinoic acid pathway regulation of vascular endothelial growth factor in ovine amnion. Reprod. Sci. 26, 1351-1359.

Clark D.E., Smith S.K., Sharkey A.M. and Charnock-Jones D.S. (1996). Localization of VEGF and expression of its receptors flt and KDR in human placenta throughout pregnancy. Hum. Reprod. 11, 1090-1098.

Coppé J.P., Desprez P.Y., Krtolica A. and Campisi J. (2010). The senescence-associated secretory phenotype: the dark side of tumor suppression. Annu. Rev. Pathol. 5, 99-118.

Dabrowski F.A., Burdzinska A., Kulesza A., Sladowska A., Zolocinska A., Gala K., Paczek L. and Wielgos M. (2017). Comparison of the paracrine activity of mesenchymal stem cells derived from human umbilical cord, amniotic membrane and adipose tissue. J. Obstet. Gynaecol. Res. 43, 1758-1768.

Druelle C., Drullion C., Deslé J., Martin N., Saas L., Cormenier J., Malaquin N., Huot L., Slomianny C., Bouali F., Vercamer C., Hot D., Pourtier A., Chevet E., Abbadie C. and Pluquet O. (2016). ATF6α regulates morphological changes associated with senescence in human fibroblasts. Oncotarget 7, 67699-67715.

Enders A.C. and King B.F. (1970). The cytology of Hofbauer cells. Anat Rec. 167, 231-236.

Eyden B. (2004). Fibroblast phenotype plasticity: relevance for understanding heterogeneity in "fibroblastic" tumors. Ultrastruct. Pathol. 28, 307-319.

Fakonti G., Pantazi P., Bokun V. and Holder B. (2022). Placental macrophage (Hofbauer Cell) responses to infection during pregnancy: A systematic scoping review. Front. Immunol. 12, 756035.

Gomez-Lopez N., Romero R., Plazyo O., Schwenkel G., Garcia-Flores V., Unkel R., Xu Y., Leng Y., Hassan S.S., Panaitescu B., Cha J. and Dey S.K. (2017). Preterm labor in the absence of acute histologic chorioamnionitis is characterized by cellular senescence of the chorioamniotic membranes. Am. J. Obstet. Gynecol. 217, e1-e17.

Gorjipour F., Hosseini Gohari L., Hajimiresmaiel S.J., Janani L., Moradi Y. and Pazoki-Toroudi H. (2021). Amniotic membrane-derived mesenchymal stem cells for heart failure: A systematic review and meta-analysis of the published preclinical studies. Med. J. Islam Repub. Iran 35, 187.

Graham C.H., Lysiak J.J., McCrae K.R. and Lala P.K. (1992). Localization of transforming growth factor-beta at the human fetal-maternal interface: role in trophoblast growth and differentiation. Biol. Reprod. 46, 561-572.

Grzywocz Z., Pius-Sadowska E., Klos P., Gryzik M., Wasilewska D., Aleksandrowicz B., Dworczynska M., Sabalinska S., Hoser G., Machalinski B. and Kawiak J. (2014). Growth factors and their receptors derived from human amniotic cells *in vitro*. Folia Histochem. Cytobiol. 52, 163-170.

Han S.S., Avery J.K. and Hale L.E. (1965). The fine structure of differentiating fibroblasts in the incisor pulp of the guinea pig. Anat. Rec. 153, 187-209.

Hoyes A.D. (1970). Ultrastructure of the mesenchymal layers of the human amnion in early pregnancy. Am. J. Obstet. Gynecol. 106, 557-566.

Hui Q., Jin Z., Li X., Liu C. and Wang X. (2018). FGF family: From drug Development to clinical application. Int. J. Mol. Sci. 19, 1875.

Ibrahim M.E., Bou-Resli M.N., Al-Zaid N.S. and Bishay L.F. (1983). Intact fetal membranes. Morphological predisposal to rupture. Acta Obstet. Gynecol. Scand. 62, 481-485.

In 't Anker P.S., Scherjon S.A., Kleijburg-van der Keur C., de Groot-Swings G.M., Claas F.H., Fibbe W.E. and Kanhai H.H. (2004). Isolation of mesenchymal stem cells of fetal or maternal origin from human placenta. Stem Cells 22, 1338-1345.

Insausti C.L., Blanquer M., Bleda P., Iniesta P., Majado M.J., Castellanos G. and Moraleda J.M. (2010). The amniotic membrane as a source of stem cells. Histol. Histopathol. 25, 91-98.

Iozzo R.V. and Schaefer L. (2015). Proteoglycan form and function: A comprehensive nomenclature of proteoglycans. Matrix Biol. 42, 11-55.

Ishida Y., Kubota H., Yamamoto A., Kitamura A., Bächinger H.P. and Nagata K. (2006). Type I collagen in Hsp47-null cells is aggregated in endoplasmic reticulum and deficient in N-propeptide processing and fibrillogenesis. Mol. Biol. Cell. 17, 2346-2355.

Jones C.J. and Fox H. (1991). Ultrastructure of the normal human placenta. Electron Microsc. Rev. 4, 129-178.

Jones C.J. and Jauniaux E. (1995). Ultrastructure of the materno-embryonic interface in the first trimester of pregnancy. Micron 26, 145-173.

Kaarteenaho-Wiik R., Paakko P. and Sormunen R. (2009). Ultrastructural features of lung fibroblast differentiation into myofibroblasts. Ultrastruct. Pathol. 33, 6-15.

Karaoz E., Aksoy A., Ayhan S., Sariboyaci A.E., Kaymaz F. and Kasap M. (2009). Characterization of mesenchymal stem cells from rat bone marrow: ultrastructural properties, differentiation potential and immunophenotypic markers. Histochem. Cell Biol. 132, 533-546.

Kii I., Nishiyama T. and Kudo A. (2016). Periostin promotes secretion of fibronectin from the endoplasmic reticulum. Biochem. Biophys. Res. Commun. 470, 888-893.

Kim S.W., Zhang H.Z., Kim C.E., An H.S., Kim J.M. and Kim M.H. (2012). Amniotic mesenchymal stem cells have robust angiogenic properties and are effective in treating hindlimb ischaemia. Cardiovasc. Res. 93, 525-534.

Kim J.H., Park S.J., Kim T.S., Park H.J., Park J., Kim B.K., Kim G.R., Kim J.M., Huang S.M., Chae J.I., Park C.K. and Lee D.S. (2013). Testicular hyperthermia induces Unfolded Protein Response signaling activation in spermatocyte. Biochem. Biophys. Res. Commun. 434, 861-866.

Kobayashi K., Inai T., Shibata Y. and Yasui M. (2009). Dynamic changes in amniotic tight junctions during pregnancy. Placenta 30, 840-847.

Koizumi N.J., Inatomi T.J., Sotozono C.J., Fullwood N.J., Quantock A.J. and Kinoshita S. (2000). Growth factor mRNA and protein in preserved human amniotic membrane. Curr. Eye Res. 20, 173-177.

Ledger P.W., Uchida N. and Tanzer M.L. (1980). Immunocytochemical localization of procollagen and fibronectin in human fibroblasts: effects of the monovalent ionophore, monensin. J. Cell. Biol. 87, 663-671.

Li L., Ly M. and Linhardt R.J. (2012). Proteoglycan sequence. Mol. Biosyst. 8, 1613-1625.

Li X., Pontén A., Aase K., Karlsson L., Abramsson A., Uutela M., Bäckström G., Hellström M., Boström H., Li H., Soriano P., Betsholtz C., Heldin C.H., Alitalo K., Ostman A. and Eriksson U. (2000). PDGF-C is a new protease-activated ligand for the PDGF alpha-receptor. Nat. Cell Biol. 2, 302-309.

Lin Y. and Xu Z. (2020). Fibroblast senescence in idiopathic pulmonary fibrosis. Front. Cell Dev. Biol. 8, 593283.

Lindquist S.L. and Kelly J.W. (2011). Chemical and biological approaches for adapting proteostasis to ameliorate protein misfolding and aggregation diseases: progress and prognosis. Cold Spring Harb. Perspect. Biol. 3, a004507.

Liong S. and Lappas M. (2014). Endoplasmic reticulum stress is increased after spontaneous labor in human fetal membranes and myometrium where it regulates the expression of prolabor mediators. Biol. Reprod. 91, 70.

Liu J., Ding Y., Liu Z. and Liang X. (2020). Senescence in mesenchymal stem cells: Functional alterations, molecular mechanisms, and rejuvenation strategies. Front. Cell Dev. Biol. 5, 258.

Lo V. and Pope E. (2009). Amniotic membrane use in dermatology. Int. J. Dermatol. 48, 935-940.

Lockwood C.J., Senyei A.E., Dische M.R., Casal D., Shah K.D., Thung S.N., Jones L., Deligdisch L. and Garite T.J. (1991). Fetal fibronectin in cervical and vaginal secretions as a predictor of preterm delivery. N. Engl. J. Med. 325, 669-674.

Lockwood C.J., Moscarelli R.D., Wein R., Lynch L., Lapinski, R.H. and Ghidini, A. (1994). Low concentrations of vaginal fetal fibronectin as a predictor of deliveries occurring after 41 weeks. Am. J. Obstet. Gynecol. 171, 1-4.

Lysiak J.J., Hunt J., Pringle G.A. and Lala P.K. (1995). Localization of transforming growth factor beta and its natural inhibitor decorin in the human placenta and decidua throughout gestation. Placenta 16, 221-231.

Lyublinskaya O., Kornienko J., Ivanova J., Pugovkina N., Alekseenko L., Lyublinskaya E., Tyuryaeva I., Smirnova I., Grinchuk T., Shorokhova M., Krasnenko A., Plotnikov N. and Nikolsky N. (2021). Induction of premature cell senescence stimulated by high doses of antioxidants is mediated by endoplasmic reticulum stress. Int. J. Mol. Sci. 22, 11851.

Majore I., Moretti P., Hass R. and Kasper C. (2009). Identification of subpopulations in mesenchymal stem cell-like cultures from human umbilical cord. Cell. Commun. Signal. 7, 6.

Malak T.M., Ockleford C.D., Bell S.C., Dalgleish R., Bright N. and Macvicar, J. (1993). Confocal immunofluorescence localization of collagen types I, III, IV, V and VI and their ultrastructural organization in term human fetal membranes. Placenta 14, 385-406.

Malhotra J.D. and Kaufman R.J. (2007). Endoplasmic reticulum stress and oxidative stress: a vicious cycle or a double-edged sword? Antioxid. Redox. Signal. 9, 2277-2293.

McParland P.C., Taylor D.J. and Bell S.C. (2000). Myofibroblast differentiation in the connective tissues of the amnion and chorion of term human fetal membranes-implications for fetal membrane rupture and labour. Placenta 21, 44-53.

Méhats C., Schmitz T., Marcellin L. and Breuiller-Fouché M. (2011). Biochemistry of fetal membranes rupture. Gynecol. Obstet. Fertil. 39, 365-369 (in French).

Meinert M., Eriksen G.V., Petersen A.C., Helmig R.B., Laurent C., Uldbjerg N. and Malmström A. (2001). Proteoglycans and hyaluronan in human fetal membranes. Am. J. Obstet. Gynecol. 184, 679-685.

Mendez M.G., Kojima S. and Goldman R.D. (2010). Vimentin induces changes in cell shape, motility, and adhesion during the epithelial to mesenchymal transition. FASEB J. 24, 1838-1851.

Menon R. (2016). Human fetal membranes at term: Dead tissue or signalers of parturition? Placenta 44, 1-5.

Menon R., Behnia F., Polettini J. and Richardson L.S. (2020). Novel pathways of inflammation in human fetal membranes associated with preterm birth and preterm pre-labor rupture of the membranes. Semin. Immunopathol. 42, 431-450.

Mezzenga R. and Mitsi M. (2019). The molecular dance of fibronectin: Conformational flexibility leads to functional versatility. Biomacromolecules 20, 55-72.

Mihu C.M., Rus Ciucă D., Soritău O., Suşman S. and Mihu D. (2009). Isolation and characterization of mesenchymal stem cells from the amniotic membrane. Rom. J. Morphol. Embryol. 50, 73-77.

Mikami T. and Kitagawa H. (2013). Biosynthesis and function of chondroitin sulfate. Biochim. Biophys. Acta 1830, 4719-4733.

Mogami H., Kishore A.H., Shi H., Keller P.W., Akgul Y. and Word R.A. (2013). Fetal fibronectin signaling induces matrix metalloproteases

and cyclooxygenase-2 (COX-2) in amnion cells and preterm birth in mice. J. Biol. Chem. 288, 1953-1966.

Moretti L., Stalfort J., Barker T.H. and Abebayehu D. (2022). The interplay of fibroblasts, the extracellular matrix, and inflammation in scar formation. J. Biol. Chem. 298, 101530.

Nickel W. and Rabouille C. (2009). Mechanisms of regulated unconventional protein secretion. Nat. Rev. Mol. Cell. Biol. 10, 148-155.

Ockleford C., Bright N., Hubbard A., D'Lacey C., Smith J., Gardiner L. Sheikh T., Albentosa M. and Turtle K. (1993). Micro-trabeculae, macro-plaques or mini-basement membranes in human term fetal membranes? Philos. Trans. R. Soc. Lond. B Biol. Sci. 342, 121-136.

Olden K., Hunter V.A. and Yamada K.M. (1980). Biosynthetic processing of the oligosaccharide chains of cellular fibronectin. Biochim. Biophys. Acta 632, 408-416.

Ostrowska-Podhorodecka Z., Ding I., Norouzi M. and McCulloch C.A. (2022). Impact of vimentin on regulation of cell signaling and matrix remodeling. Front. Cell Dev. Biol. 10, 869069.

Papp S., Fadel M.P., Kim H., McCulloch C.A. and Opas M. (2007). Calreticulin affects fibronectin-based cell-substratum adhesion via the regulation of c-Src activity. J. Biol. Chem. 282, 16585-16598.

Parolini O., Alviano F., Bagnara G.P., Bilic G., Bühring H.J., Evangelista M., Hennerbichler S., Liu B., Magatti M., Mao N., Miki T., Marongiu F., Nakajima H., Nikaido T., Portmann-Lanz C.B., Sankar V., Soncini M., Stadler G., Surbek D., Takahashi T.A., Redl H., Sakuragawa N., Wolbank S., Zeisberger S., Zisch A. and Strom S.C. (2008). Concise review: isolation and characterization of cells from human term placenta: outcome of the first international Workshop on Placenta Derived Stem Cells. Stem Cells 26, 300-311.

Pasquinelli G., Tazzari P., Ricci F., Vaselli C., Buzzi M., Conte R., Orrico C., Foroni L., Stella A., Alviano F., Bagnara G.P. and Lucarelli E. (2007). Ultrastructural characteristics of human mesenchymal stromal (stem) cells derived from bone marrow and term placenta. Ultrastruct. Pathol. 31, 23-31.

Paul G., Özen I, Christophersen N.S., Reinbothe T., Bengzon, J., Visse E., Jansson K., Dannaeus K., Henriques-Oliveira C., Roybon L., Anisimov S.V., Renström E., Svensson M., Haegerstrand A. and Brundin P. (2012). The adult human brain harbors multipotent perivascular mesenchymal stem cells. PLoS One 7, e35577.

Paulin D., Lilienbaum A., Kardjian S., Agbulut O. and Li Z. (2022). Vimentin: Regulation and pathogenesis. Biochimie 197, 96-112.

Pinart E., Bonet S., Briz M., Pastor L.M., Sancho S., García N., Badia E. and Bassols J. (2001). Lectin affinity of the seminiferous epithelium in healthy and cryptorchid post-pubertal boars. Int. J. Androl. 24, 153-164

Pluquet O., Pourtier A. and Abbadie C. (2015). The unfolded protein response and cellular senescence. A review in the theme: cellular mechanisms of endoplasmic reticulum stress signaling in health and disease. Am. J. Physiol. Cell Physiol. 308, C415-425.

Portmann-Lanz C.B., Schoeberlein A., Huber A., Sager R., Malek A., Holzgreve W. and Surbek D.V. (2006). Placental mesenchymal stem cells as potential autologous graft for pre- and perinatal neuroregeneration. Am. J. Obstet. Gynecol. 194, 664-673.

Ross R. and Benditt E.P. (1965). Wound healing and collagen formation. V. Quantitative electron microscope radioautographic observations of proline-H3 utilization by fibroblasts. J. Cell Biol. 27, 83-106.

Ross R. (1975). Connective tissue cells, cell proliferation and synthesis of extracellular matrix - a review. Philos. Trans. R. Soc. Lond. B Biol. Sci. 271, 247-259.

Rylova Y.V., Milovanova N.V., Gordeeva M.N. and Savilova A.M. (2015). Characteristics of multipotent mesenchymal stromal cells from human terminal placenta. Bull. Exp. Bio.l Med. 159, 253-257.

Schilling B. and Yeh J. (2000). Transforming growth factor-beta(1), -beta(2), -beta(3) and their type I and II receptors in human term placenta. Gynecol. Obstet. Invest. 50, 19-23.

Sessarego N., Parodi A., Podestà M., Benvenuto F., Mogni M., Raviolo V., Lituania M., Kunkl A., Ferlazzo G., Bricarelli F.D., Uccelli A. And Frassoni F. (2008). Multipotent mesenchymal stromal cells from amniotic fluid: solid perspectives for clinical application. Haematologica 93, 339-346.

Shaer A., Azarpira N., Aghdaie M.H. and Esfandiari E. (2014). Isolation and characterization of human mesenchymal stromal cells derived from placental decidua basalis; Umbilical cord Wharton's Jelly and amniotic membrane. Pak. J. Med. Sci. 30, 1022-1026.

Shen T., Xia L., Dong W., Wang J., Su F., Niu S., Wang Q. and Fang Y. (2021). A systematic review and meta-analysis: Safety and efficacy of mesenchymal stem cells therapy for heart failure. Curr. Stem Cell Res. Ther. 16, 354-365.

Strauss J.F. (2013). Extracellular matrix dynamics and fetal membrane rupture. Reprod. Sci. 20, 140-153.

Strueby L. and Thébaud B. (2016). Mesenchymal stromal cell-based therapies for chronic lung disease of prematurity. Am. J. Perinatol. 33, 1043-1049.

Takechi K., Kuwabara Y. and Mizuno M. (1993). Ultrastructural and immunohistochemical studies of Wharton's jelly umbilical cord cells. Placenta 14, 235-245.

Takii M., Suehiro T., Shima A., Yotsueda H., Hisano S. and Katafuchi R. (2017). Fibronectin glomerulopathy complicated with persistent cloaca and congenital esophageal atresia: a case report and literature review. BMC Nephrol. 18, 288.

Tang K., Wu J., Xiong Z., Ji Y., Sun T. and Guo X. (2018). Human acellular amniotic membrane: A potential osteoinductive biomaterial for bone regeneration. J. Biomater. Appl. 32, 754-764.

Tavasolian F., Hosseini A.Z., Mirzaei A., Abdollahi E., Jandaghi P., Soudi S., Naderi M., Saburi E., Momtazi-Borojeni A.A., Johnston T.P. and Sahebkar A. (2020). Unfolded protein response-mediated modulation of mesenchymal stem cells. IUBMB Life 72, 187-197.

Tian J., Lei X.X., Xuan L., Tang J.B. and Cheng B. (2019). The effects of aging, diabetes mellitus, and antiplatelet drugs on growth factors and anti-aging proteins in platelet-rich plasma. Platelets 30, 773-792.

Toda A., Okabe M., Yoshida T. and Nikaido T. (2007). The potential of amniotic membrane/amnion-derived cells for regeneration of various tissues. J. Pharmacol. Sci. 105, 215-228.

Tomasek J.J., Gabbiani G., Hinz B., Chaponnier C. and Brown R.A. (2002). Myofibroblasts and mechano-regulation of connective tissue remodelling. Nat. Rev. Mol. Cell. Biol. 3, 349-363.

Tumbar T., Guasch G., Greco V., Blanpain C., Lowry W.E., Rendl M. and Fuchs E. (2004). Defining the epithelial stem cell niche in skin. Science 303, 359-363.

van Bekkum D.W., van Noord M.J., Maat B. and Dicke K.A. (1971). Attempts at identification of hemopoietic stem cell in mouse. Blood 38, 547-558.

Veerbeek J.H., Tissot Van Patot M.C., Burton G.J. and Yung H.W. (2015). Endoplasmic reticulum stress is induced in the human placenta during labour. Placenta 36, 88-92.

Vellasamy S., Sandrasaigaran P., Vidyadaran S., George E. and Ramasamy R. (2012). Isolation and characterisation of

mesenchymal stem cells derived from human placenta tissue. World J. Stem Cells 4, 53-61.

Vestentoft P.S. (2013). Development and molecular composition of the hepatic progenitor cell niche. Dan. Med. J. 60, B4640.

Vitellaro-Zuccarello L., Dyne K. and Cetta G. (1989). Biochemical, morphological and stereological study of the dermis in three members of a large family with type IV Ehlers-Danlos syndrome. Connect. Tissue Res. 23, 1-17.

Yoshino I., Kometani T., Shoji F., Osoegawa A., Ohba T., Kouso H., Takenaka T., Yohena T. and Maehara Y. (2007). Induction of epithelial-mesenchymal transition-related genes by benzo[a]pyrene in lung cancer cells. Cancer 110, 369-374.

Yung H.W., Calabrese S., Hynx D., Hemmings B.A., Cetin I., Charnock-Jones D.S. and Burton, G.J. (2008). Evidence of placental translation inhibition and endoplasmic reticulum stress in the etiology of human intrauterine growth restriction. Am. J. Pathol. 173, 451-462.

Zhu B.C., Fisher S.F., Pande H., Calaycay J., Shively J.E. and Laine R.A. (1984). Human placental (fetal) fibronectin: increased glycosylation and higher protease resistance than plasma fibronectin. Presence of polylactosamine glycopeptides and properties of a 44-kilodalton chymotryptic collagen-binding domain: difference from human plasma fibronectin. J. Biol. Chem. 259, 3962-3970.

Accepted September 4, 2023